

**THE USE OF BORON-CONTAINING ADDITIVES  
FOR SYNTHESIS OF ANORTHITE  
CERAMIC POWDERS**

**A Thesis Submitted to  
the Graduate School of Engineering and Sciences of  
İzmir Institute of Technology  
in Partial Fulfillment of the Requirements for the Degree of**

**MASTER OF SCIENCE**

**In Materials Science and Engineering**

**by  
Sedat KAVALCI**

**July 2006  
İZMİR**

We approve the thesis of **Sedat KAVALCI**

**Date of Signature**

.....  
**Assoc. Prof. Dr. Sedat AKKURT**  
Supervisor  
Department of Mechanical Engineering  
İzmir Institute of Technology

**18.07.2006**

.....  
**Prof. Dr. Muhsin ÇİFTÇİOĞLU**  
Co-Supervisor  
Department of Chemical Engineering  
İzmir Institute of Technology

**18.07.2006**

.....  
**Assoc. Prof. Dr. Mustafa GÜDEN**  
Department of Mechanical Engineering  
İzmir Institute of Technology

**18.07.2006**

.....  
**Asst. Prof. Dr. Figen TOKATLI**  
Department of Food Engineering  
İzmir Institute of Technology

**18.07.2006**

.....  
**Asst. Prof. Dr. Mehtap EMİRDAĞ EANES**  
Department of Chemistry  
İzmir Institute of Technology

**18.07.2006**

.....  
**Prof. Dr. Muhsin ÇİFTÇİOĞLU**  
Head of Interdisciplinary  
Materials Science and Engineering Program  
İzmir Institute of Technology

**18.07.2006**

.....  
**Assoc. Prof. Dr. Semahat ÖZDEMİR**  
Head of the Graduate School

## **ACKNOWLEDGEMENTS**

I would like to express my gratitude to my advisor, Assoc. Prof. Sedat AKKURT for his supervision, guidance and encouragement throughout study.

I am also grateful to IYTE-CMR staff for their technical support.

I would like to appreciate deeply to Mücahit SÜTÇÜ, EMRE YALAMAÇ and friends for their support and help.

Finally, I would like to thank my family for their support and encouragement.

## ABSTRACT

### THE USE OF BORON-CONTAINING ADDITIVES FOR SYNTHESIS OF ANORTHITE CERAMIC POWDERS

Anorthite ceramics have a great potential as a substrate material due to their low thermal expansion coefficient and low dielectric constant. For lowering the sintering temperature of anorthite ceramics several routes like employing additives, sol-gel method and the use of mechanochemical methods have been proposed.

In this study, anorthite was synthesized by using mechanochemical methods and boron oxide addition. The raw materials used in this study were Sivas kaolin as a source for  $\text{Al}_2\text{O}_3$  and  $\text{SiO}_2$ , calcined alumina or  $\text{Al}(\text{OH})_3$  as a source for  $\text{Al}_2\text{O}_3$  and calcite powder as source for  $\text{CaO}$ . Phase characterizations of synthesized powders were performed by XRD using  $\text{CuK}\alpha$  radiation. Microstructural characterization was performed by SEM. Statistical experimental design techniques (SED) were used in order to determine and analyze the more important process variables for synthesizing anorthite ceramics.

The results of screening experimental design clarified that the temperature was the most important process variable. Second most important process variable was grinding speed which was followed by additive amount and additive type. This study showed that both additive type and additive amount were important process variables because these two factors were related to each other.

The effect of both additive use and grinding on anorthite synthesis helped decrease the synthesis temperature down to  $900\text{ }^\circ\text{C}$ .

# ÖZET

## BORON İÇEREN KATKILARI KULLANARAK ANORTİT SERAMİK TOZU SENTEZLENMESİ

Anortit seramikleri devre altlığı malzemesi olarak sahip oldukları düşük ısıl genleşme ve düşük elektriksel katsayıları nedeniyle büyük potansiyele sahiptirler. Anortit seramiklerinin sinterleme sıcaklığını düşürmek için katkı eklemek, sol-gel yöntemi ve mekanokimyasal yöntemler kullanmak gibi birkaç yöntem önerilmiştir.

Bu çalışmada anortit mekanokimyasal yöntemler ve boron ilavesi ile sentezlenmiştir. Bu çalışmada kullanılan sarf malzemeler; Sivas kaolin ( $Al_2O_3$  ve  $SiO_2$  kaynağı olarak), kalsine edilmiş alumina veya  $Al(OH)_3$  (alumina kaynağı olarak) ve kalsiyum karbonat tozu ( $CaO$  kaynağı olarak) kullanılmıştır. Sentezlenen tozların faz karakterizasyonu X-Işını Kırınımı (XRD) ile  $CuK\alpha$  radyasyonu kullanılarak yapılmıştır. Mikro yapı karakterizasyonu için taramalı elektron mikroskobu (SEM) kullanılmıştır. Anortit seramik sentezlemesinde daha önemli olan proses değişkenlerini belirlemek ve analiz etmek için istatistiksel deney dizaynı (SED) kullanılmıştır.

Eleme deneysel tasarımının sonuçları göstermiştir ki sıcaklık en önemli proses değişkenidir. İkinci en önemli proses değişkeni ise öğütme süresidir. Bunu katkı miktarı ve katkı cinsi takip etmektedir. Bu çalışma göstermiştir ki katkı miktarı ve katkı cinsi önemli proses değişkenleridir. Bunun nedeni bu iki proses değişkeninin birbirine bağımlı olmasındandır.

Katkı kullanımı ve öğütmenin birlikte etkilerinin anortit sentezi üzerindeki etkileri sayesinde sentezleme sıcaklığı  $900\text{ }^\circ\text{C}$ 'ye kadar indirilmiştir.

# TABLE OF CONTENTS

LIST OF FIGURES .....	viii
LIST OF TABLES .....	ix
CHAPTER 1. INTRODUCTION .....	1
CHAPTER 2. LITERATURE SURVEY .....	3
2.1. Mechanochemisrty .....	3
2.2. Anorthite .....	4
2.2.1. Anorthite synthesis .....	6
2.2.2. CaO-Al <sub>2</sub> O <sub>3</sub> -SiO <sub>2</sub> System.....	11
CHAPTER 3. EXPERIMENTAL.....	13
3.1. Materials .....	13
3.2. Methods .....	16
3.2.1. Powder Mixture Preparation.....	16
3.2.2. Grinding .....	18
3.2.3. Compaction.....	18
3.2.4. Heat Treatment .....	18
3.3. Product Analysis .....	19
3.3.1. X-Ray Diffraction Analyses .....	19
3.3.2. Microstructural Analyses (SEM).....	20
3.3.3. Density and Porosity Measurements.....	20
3.4. Statistical Experimental Design.....	20
3.4.1. Fractional Factorial Design.....	21
3.4.1.1. Plackett Burman Screening Design .....	22
3.4.1.2. Response Surface Design.....	24

CHAPTER 4. RESULTS AND DISCUSSION.....	29
4.1. Anorthite Synthesis.....	29
4.1.1. Labelling System Used for Samples in Cordierite Synthesis .....	29
4.1.2. Results of Plackett-Burman Screening Design for Anorthite Synthesis .....	30
4.1.3. Results of Box-Behnken Response Surface Design for Anorthite Synthesis.....	37
4.1.4. Effect of Grinding Speed and Temperature on Anorthite Synthesis .....	46
4.1.5. Effect of Alumina Source on Anorthite Synthesis.....	49
4.1.6. Effect of Grinding Time on Anorthite Synthesis.....	50
4.2. Microstructural Evaluation .....	51
4.3. Density and Porosity Evaluation.....	53
 CHAPTER 5. CONCLUSION.....	 55
 REFERENCES .....	 57

## LIST OF FIGURES

<b><u>Figure</u></b>		<b><u>Page</u></b>
Figure 2.1.	Composition range of most natural feldspars .....	5
Figure 2.2.	The structure of anorthite.....	5
Figure 2.3.	CaO-Al <sub>2</sub> O <sub>3</sub> -SiO <sub>2</sub> ternary phase diagram.....	12
Figure 3.1.	X-ray analysis of raw material Sivas Kaolin .....	14
Figure 3.2.	Schematic drawing showing the main steps of sample preparation .....	17
Figure 3.3.	Planetary mono mill.....	18
Figure 3.4.	Globar benchtop kiln .....	19
Figure 3.5.	Box-Behnken design for three factors .....	27
Figure 3.6.	Geometrical structure of Box-Behnken design for three factors .....	28
Figure 4.1.	XRD patterns of the screening design samples .....	31
Figure 4.2.	Half-Normal probability plot of the effects for the Plackett-Burmann design .....	34
Figure 4.3.	XRD patterns of the Box-Behnken response surface design (1) .....	39
Figure 4.4.	XRD patterns of the Box-Behnken response surface design (2) .....	40
Figure 4.5.	Normal probability plot for Box-Behnken design .....	41
Figure 4.6.	Predicted values ( $\hat{y}$ ) vs observed values (y).....	44
Figure 4.7.	Response surfaces and design cube .....	45
Figure 4.8.	The XRD patterns of samples fired at 800 oC that were ground at different speeds .....	47
Figure 4.9.	The XRD patterns of samples fired at 900 oC that were ground at different speeds .....	48
Figure 4.10.	The XRD patterns of samples fired at 1100 oC that were ground at different speeds .....	48
Figure 4.11.	The XRD patterns of samples that had different Al <sub>2</sub> O <sub>3</sub> sources.....	50
Figure 4.12.	The XRD patterns of samples that were ground for different grinding durations .....	51
Figure 4.13.	SEM micrographs of specimens heated at different temperatures and soak times.....	52
Figure 4.14.	SEM micrographs of sample R13-B-3-1000-1-45-500 .....	52
Figure 4.15.	SEM micrographs of sample R6-B-3-1100-1-15-500 .....	53

## LIST OF TABLES

<b>Table</b>	<b>Page</b>
Table 2.1. Main physical properties of anorthite .....	6
Table 3.1. Chemical analyses of the raw materials and additives .....	15
Table 3.2. Physical properties of as-received raw materials and additives .....	16
Table 3.3. The amounts of raw materials and additives for mixtures.....	17
Table 3.4. JCPDS card number and peak positions used for XRD peak intensity Measurements .....	19
Table 3.5. Distribution of degree of freedoms for 26 design.....	21
Table 3.6. Plus and minus signs for the first rows of the Plackett-Burman designs .....	22
Table 3.7. Design set of experiments for Plackett-Burman design with 12 runs.....	23
Table 3.8. The factors for Plackett-Burman screening design.....	24
Table 3.9. Required number of run points in three level factorial design .....	26
Table 3.10. The coded levels of independent variables for three variable Box- Behnken design.....	28
Table 4.1. Evaluation of Plankett-Burmann design.....	34
Table 4.2. ANOVA table for the Plankett-Burmann screening design.....	36
Table 4.3. Design Expert 7.0. software output for the Plackett-Burmann screening design.....	37
Table 4.4. The actual values of factors for Box-Behnken response surface design .....	38
Table 4.5. The responses of experiments for Box-Behnken design .....	41
Table 4.6. ANOVA table for the Box-Behnken response surface design .....	42
Table 4.7. Design Expert 7.0. software output for Box-Behnken response surface design .....	43
Table 4.8. The levels of factors at the optimum operation point .....	46
Table 4.9. Samples studied for effect of grinding analysis.....	46
Table 4.10. Archimedes density of anorthite pellets.....	54

# CHAPTER 1

## INTRODUCTION

The electronic industry demands more integrated, smaller and faster circuits which require new materials. Two properties are important for integrated circuit substrate applications. One is thermal expansion coefficient and the other is dielectric constant. The mismatch in thermal expansion coefficient between substrate and chip causes stresses in the chip-to-substrate ceramic joints which is an important problem for reducing the size of integrated circuits (ex:  $\alpha_{\text{Si}} = 26 \times 10^{-7}/^{\circ}\text{C}$  while  $\alpha_{\text{Al}_2\text{O}_3} = 72 \times 10^{-7}/^{\circ}\text{C}$ ). Also, faster circuitry requires as low a dielectric constant as possible to reduce the delay times for increasing the processing speed in circuitry. Today's common substrate material is alumina with dielectric constant  $\epsilon_r \approx 9$  at 1 MHz which can not perfectly satisfy the demands. Another desired property for substrate application is low sintering temperature of around 1000 °C. In other words sintering temperature should be lower than the melting temperature of common conductive metals like copper, silver and gold. This enables the substrate to co-fire with the conductive metals (Gdula 1971).

Anorthite ( $\text{CaO} \cdot \text{Al}_2\text{O}_3 \cdot 2\text{SiO}_2$ ) which is the lime-rich end member of plagioclase feldspar solid solution, has great potential as a ceramic material for electronic substrate applications because of its low thermal expansion coefficient  $45 \times 10^{-7}/^{\circ}\text{C}$ , (between 25-1000°C) and low dielectric constant ( $\epsilon_r \approx 6.2$  at 1 MHz). The natural anorthite is a rare material that can not be mined in mass tonnages and also the quality of the material does not satisfy the industrial demand. So, anorthite should be synthetically produced from inexpensive raw materials.

Anorthite had been investigated by many researchers and they had proposed several routes for synthesizing anorthite for decreasing the sintering temperature and improving physical properties such as density (Gdula 1971, Mergen and Aslanoğlu 2003, Mergen et. al. 2004, Kobayashi and Kato 1994, Lee and Kim 2002, Yang and Cheng 1998, Yang and Cheng 1999, Boudchicha 2001, Guechi 2004, Okada et. al. 2003, Traoré et. al. 2003). Some of these methods were; intensive mechanical grinding, synthesizing by sol-gel method, employing different nucleating agents like  $\text{TiO}_2$ ,  $\text{B}_2\text{O}_3$ ,  $\text{Na}_2\text{CO}_3$  and using different raw materials. All these methods carry their own

advantages and disadvantages. In this study, anorthite was synthesized by employing mechanical grinding and using boron containing additives.

Mechanical grinding activates the reactivity of solids by mechanical means which are frictional and impact forces. Mechanical grinding procedures have advantages over the traditional technological methods. Mechanical grinding simplifies the process by decreasing the number of process stages, and it is relatively environmentally friendly because it does not need any chemical solvents. Main advantages of mechanical grinding are decreases in the sintering temperature, increases in the reaction rate of particles, reduces the particle size, increases strain (decreases the amount of energy needed for sintering), enables obtaining denser bodies, increases specific surface area and increases homogeneity of compounds in the powder (Kostic et al. 1997).

The use of additives for lowering the sintering temperature is a well known method for producing denser ceramics. The additives are basically materials which have lower melting temperature than the sintering temperature and they do not take part in chemical reactions during the sintering process. As additives melt they form a liquid network between the components and increase the diffusion rate between them. Also they act as grain growth inhibitors (Kingery 1975). Boron containing sintering aids like colemanite ( $2\text{CaO}\cdot 3\text{B}_2\text{O}_3\cdot 5\text{H}_2\text{O}$ ) and boric acid ( $\text{H}_3\text{BO}_3$ ) are used to decrease the sintering temperature and to increase the density of anorthite. The boron containing additives are chosen because they have low melting point and have less harmful effect on insulating characteristics of anorthite than other sintering aids (Mergen and Aslanoğlu 2003).

The experiments were planned by the use of statistical experimental design techniques (SED). First, screening experimental design was employed to separate the more important factor effects for full factorial design. Secondly, response surface design was employed to understand the effects of process variables on the amount of synthesized product. Finally ladder experiments were performed to understand the effects of grinding time, grinding speed and the type of additives on the success of anorthite synthesis.

In the second chapter of this thesis the information collected from the literature on the production of anorthite is presented. The third chapter shows the experimental work conducted and the fourth chapter gives results obtained from the experiments. Finally the conclusions are given in the fifth chapter.

## CHAPTER 2

### LITERATURE SURVEY

#### 2.1. Mechanochemistry

Mechanochemistry is concerned with chemical reactions and reactivity of solids caused by mechanical forces. The main purpose of mechanochemistry is shattering powders for increasing surface by mechanical energy (Steinike and Tkacova 2000). Mechanochemistry is the subject of increasing interest to solid state science and technology. Mechanochemical synthesis has great potential for low temperature synthesis with benefit of obtaining denser bodies (Yalamaç and Akkurt 2006). Chemical effects caused by mechanical means have very long history but the theory behind mechanochemistry was established in early 20<sup>th</sup> century. Mechanochemistry has applied on an industrial scale since 1966 and the mathematical modelling of mechanochemical process began in mid 1980s (Rojac et al. 2005).

Hydrostatic loading and shear loading and their combinations are the main mechanisms in mechanochemistry. There are several types of mechanical activators. First, shock activators in which disintegration is sustained by accelerating particles and then crushed into high speed moving blades such as high peripheral-speed pin mills and jet mills. Second type are shear activators in which shear loading is applied by moving a solid body across another and the powder is placed between these two bodies such as rollers, Leche mills. The third and the last type of activators are ball mills and vibration devices. Both shear and hydrostatic mechanical loadings are exerted to solid in these devices. The loading characteristics depend on construction designs of the mills.

The effects of mechanical deformation of solids altered their structure and physical properties such as intensive structural changes of amorphization and less intensive changes in grains. The mechanochemical changes promote easy consolidation and transformation of phases in the sintering (Sánchez et al. 2004).

In mechanochemistry, mechanical action causes the formation of strain field in the solid by shifting the atoms from their equilibrium stable positions which leads to changes of bond lengths and their angles also affecting electron subsystem. These effects create metastable states so their formation is followed by relaxation for being

stable again. Energy stored as strain field is partially converted into heat. Another way of this conversion is plastic deformation. The combination of plastic deformation and strain concentrated sites leads to disintegration of particles with increasing overall surface area. The reductions in size of crystals continue to some critical value. Further size reduction leads to amorphization of crystal structure or formation of defects inside crystal which causes transition into metastable polymorphous state. Also, relaxation of strain field results in the rupture of chemical bonds. The four processes, accumulation of defects, amorphization, formation of metastable polymorphous states, and chemical reaction, are named as mechanical activation (Boldyrev and Tkacova 2000).

## **2.2. Anorthite**

Anorthite was first reported from the Franklin Marble in the Fowler Quarry near a contact with pegmatite by Warren in 1901. Anorthite ( $\text{CaO} \cdot \text{Al}_2\text{O}_3 \cdot 2\text{SiO}_2$ ) is a lime-rich end member of the plagioclase feldspar solid solution series. “The feldspars are by far the most abundant group of minerals. They are found in nearly all igneous rocks, most metamorphic rocks, and are an important constituent in many sedimentary rocks.” (Nesse W. D. 1991). The composition of the common feldspars can be expressed in terms of three end members: K-feldspars ( $\text{KAlSi}_3\text{O}_8$ ), albite ( $\text{NaAlSi}_3\text{O}_8$ ), and anorthite ( $\text{CaAl}_2\text{Si}_2\text{O}_8$ ). Natural feldspars fall into either the plagioclase series with compositions between albite and anorthite or the alkali feldspar series with compositions between albite and K-feldspar seen in Figure 2.1. The plagioclase series comprise minerals that range in chemical composition from pure  $\text{NaAlSi}_3\text{O}_8$ , albite to pure  $\text{CaAl}_2\text{Si}_2\text{O}_8$ , anorthite. For natural anorthite by definition must contain no more than 10% sodium and no less than 90% calcium in the sodium/calcium position in the crystal structure. Some of main physical properties are given in Table 2.1.

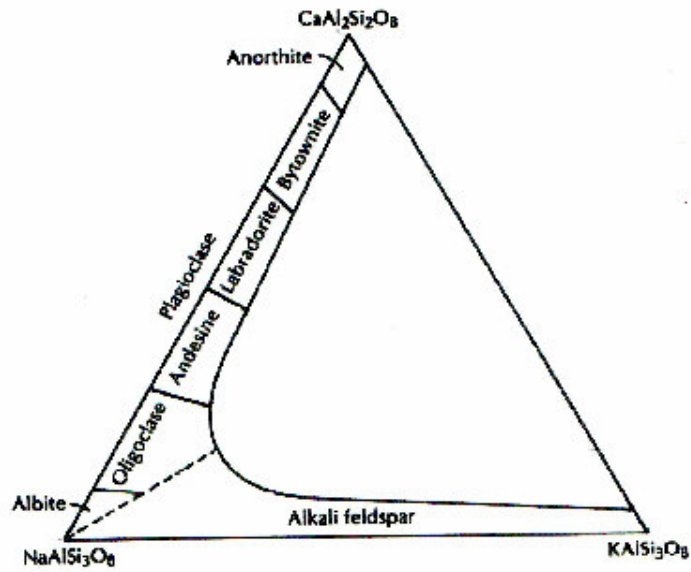


Figure 2.1. Composition range of most natural feldspars  
(Source: Nesse W. D., 1991)

Natural anorthite mineral shows triclinic symmetry and is composed of frame work of (Si,Al)-O tetrahedra with  $\text{Ca}^{+2}$  ions settled in an interstice, which is shown in Figure 2.2 (Deer et al. 1963). There is one interstices for each for tetrahedra and half of the tetrahedra is occupied by  $\text{Al}^{+3}$  ions.

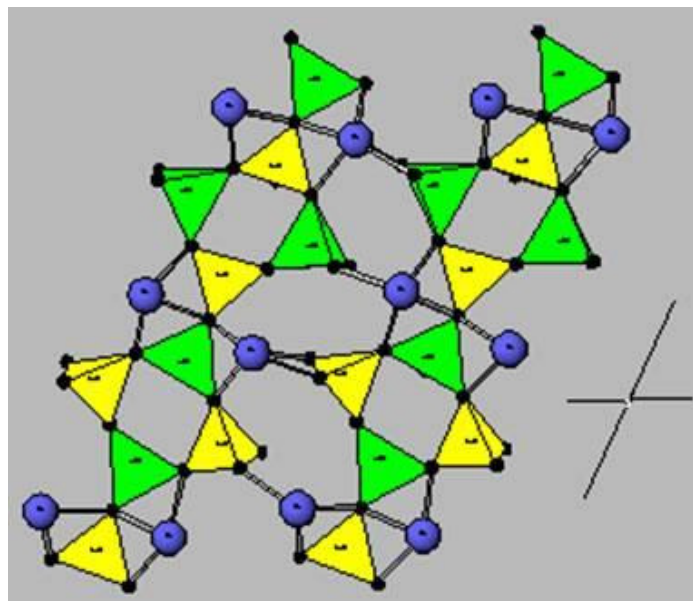


Figure 2.2. The structure of anorthite  
(Source: WEB\_1, 2006.)

Table 2.1. Main physical properties of anorthite

<b>T<sub>melting</sub></b> (°C)	<b>Density</b> (g/cm <sup>3</sup> )	<b>Crystal structure</b>	<b>Refractive index</b>	<b>Lattice angles</b>	<b>Lattice constant</b> (Å)	<b>Molecular Weight</b> (g)
1553	2.76	Orthorhombic & Hexagonal	1.575 to 1.591	$\alpha=93.17^\circ$ $\beta=115.91^\circ$ $\gamma=91.20^\circ$	a = 8.17 b = 12.87 c = 14.18	158.08

Anorthite has thermal expansion coefficient  $45 \times 10^{-7}/^\circ\text{C}$  (between 25-1000°C), dielectric constant  $\epsilon_r \approx 6.2$  (at 1 MHz) and volume resistivity of  $2.8 \times 10^{15} \Omega\text{cm}$  (at 25°C) and  $1.9 \times 10^{15} \Omega\text{cm}$  (at 100°C) which makes anorthite ceramics and anorthite based glass ceramics promising candidates for substrate materials in microelectronic applications. In order to be an effective substrate material, the anorthite ceramic must have sufficiently low sintering temperature such as lower than 1000°C. This property is prerequisite for co-firing substrate ceramic with conductive metals such as copper, gold and silver. Low temperature co-firing is also essential for preventing the oxidation of circuit elements during co-firing (Knickerbocker et al. 1993). Many scientists worked for lowering the sintering temperature of substrate ceramics.

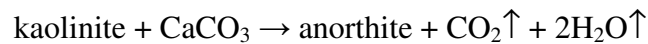
Nevertheless, anorthite can not be mined in mass tonnage quantities. So, it must be synthetically produced. For this purpose various sintering techniques were established. These techniques are briefly presented in this section. In the next section, studies for mechanochemical synthesis of anorthite are explained.

### 2.2.1. Anorthite Synthesis

As mentioned in previous section, anorthite is a promising ceramic material for electronic applications. Anorthite production techniques have been the subject of extensive research. Techniques for anorthite synthesis include sintering of solid mixtures of calcium carbonate, kaolinite, alumina, and aluminum hydroxide in addition to mechanochemical treatments, sol-gel process of dehydration of appropriate metal

hydroxides , or employing different additives in solid state sintering process such as  $B_2O_3$ ,  $Na_2CO_3$ ,  $TiO_2$ ,  $CaF_2$  .

One of the earliest studies about anorthite by R.A.Gdula represented the electrical properties of anorthite for substrate applications in electronic devices. The raw materials are kaolinite and  $CaCO_3$ . The proposed reaction is:



The mixture was wet milled for 2 hours with alumina mills. The slurry was dried and calcined at  $1100^\circ C$  with a heating regime of  $250^\circ C/h$  for 18 hours. The calcined body was dry ball-milled for 16 hours with grinding aid of 1 wt% polyethylene glycol and then pressed in pellets and sintered at  $1450^\circ C$  for 2 hours. The study resulted in anorthite ceramics which were suitable for dielectric applications due to its low thermal expansion coefficient and low dielectric constant. Furthermore, the raw materials were inexpensive and the production process was simple and straightforward (Gdula 1971).

Mergen and Aslanoğlu, employed the additive of boron oxide for lowering the sintering temperature for anorthite ceramics. The raw materials were Goleg kaolinite (China), quartz and calcite. The mean particle sizes for kaolinite and calcite were 5 and 18  $\mu m$  respectively. The mixture prepared by mixing stoichiometric amounts of kaolinite, quartz and calcite with 3 wt%  $B_2O_3$  as  $H_3BO_3$  were wet milled in deionized water for 4 hours using alumina balls in plastic container. The slurry was dried for 24 hours at  $80^\circ C$  and pressed into pellets of 10 mm diameter at 70 MPa. The pellets sintered at a temperature range of  $950^\circ C$  to  $1000^\circ C$  for 1 hour. The heating and cooling rate was fixed to  $300^\circ C/h$ . They concluded that boron addition leads to the formation of single anorthite phase at low temperatures. They achieved to synthesize anorthite at  $950^\circ C$  with 87% of theoretical density without using fine raw materials (Mergen and Aslanoğlu 2003).

In a more recent study of Mergen et al., they investigated the affect of another boron containing additive; colemanite ( $2CaO.3B_2O_3.5H_2O$ ). They used domestic impure kaolinite, calcite and quartz as raw materials which were relatively coarse. Three weight percent boron oxide was added as colemanite. The stoichiometric mixture, calculated according to anorthite phase, and additive wet milled for 5 hours with alumina balls in plastic container. The slurry was dried and pellets were pressed at 80 MPa with a

diameter of 25 mm. The pellets were fired in air in the range of 900 -1400°C for 1 hour. They concluded that colemanite addition accelerated the formation of anorthite phase. The bulk density of the sintered ceramics at 1350°C with colemanite addition reached 91.3% theoretical density. On the other hand, the batches without additive only reached 73.5% of theoretical density at the same sintering temperature and process conditions (Mergen et al. 2004).

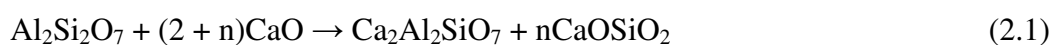
In another study, Cheng-Fu Yang et al. investigated the sintering characteristics of MgO-CaO-Al<sub>2</sub>O<sub>3</sub>-SiO<sub>2</sub> (MCAS) composite glass powders. They used sol-gel process in which the appropriate metal hydroxides mixed. The dehydration of this mixture resulted in a homogenous mixture of metal oxides. Colloidal silica was dispersed in deionized water and concentrated nitric acid. Addition of magnesium nitrate hexahydrate, aluminum nitrate hexahydrate, calcium nitrate hexahydrate and ammonium hydroxide to this mixture resulted in the quantitative precipitation of magnesium, aluminum and calcium hydroxides. Filtration is used for collecting the solid particles. The particles were calcined at 300°C for 1 hour. This calcination step was necessary for converting the remaining ammonium nitrate to nitrogen and water. The samples were sintered at temperatures of 800 to 1000°C for soaking time of 40 minutes. Also, the effect of soaking time was investigated. For this purpose some of the samples were sintered at 940°C for 20-360 minutes. They reported that the sintered density increases with temperature up to 1000°C. They also concluded that if the sintering temperature of the samples was high enough the soaking time becomes more important factor than sintering temperature to improve recrystallization (Yang and Cheng 1998).

In another study Yang et al., investigated the influence of B<sub>2</sub>O<sub>3</sub> on the sintering characteristics the MgO-CaO-Al<sub>2</sub>O<sub>3</sub>-SiO<sub>2</sub> (MCAS) composite glass powders. They used sol-gel process which is also mentioned above. The B<sub>2</sub>O<sub>3</sub> was added to this mixture by slurry method as 0 wt%, 1 wt%, 3 wt% and 6 wt%. The sintering temperature was varied in the range from 800°C to 1000°C with a heating rate of 5°C/min. They concluded that the increase in the B<sub>2</sub>O<sub>3</sub> amount promoted the densification, decreased the sintering temperature and resulted in pore elimination. However, addition of too much B<sub>2</sub>O<sub>3</sub> inhibited the crystallization rates of the MCAS composite glass powders (Yang and Cheng 1999).

Another synthesis method similar to the sol-gel method is solution process. Lee and Kim studied the densification behavior of anorthite by employing polymer carrier.

This process had the basic idea that using hydroxycarboxylic acid such as citric and lactic acid with polyhydroxyl alcohol (i.e. ethylene glycol) to form condensation reactions. The hydroxycarboxylic acid acted as chelating agent which chemically bound to the cations that were dissolved in the solution. The polymerization was based on the polyesterification between metal-chelate complexes and polyhydroxyl alcohols. Because of the chelating action of hydroxycarboxylic acids with polymeric network, the cations had low mobility. So, precipitation was hindered which results in better chemical homogeneity and smaller particle size. In this study, polyvinyl alcohol (PVA) was used as polymer carrier because of its simple structure and its low price. The PVA operated as steric entrapment mechanism in the organic-inorganic solution because of its large chain molecule. The degree of polymerization, degree of hydrolysis and the assignment of the hydrolyzed groups determined the properties of PVA. Calcium nitrate, aluminum nitrate and colloidal silica solution were dissolved in stoichiometric amounts in deionized water. Next, 5 wt% polyvinyl alcohol (PVA) added to this solution. Water evaporated by continuous stirring on a hot plate. The resultant powder was planetary ball-milled at 200 rpm for 20 hours in a zirconia media. The powder wet milled with addition of iso-propyl alcohol. The powder pressed into pellets and fired between 900°C to 1000°C for 1 hour with a heating rate of 4 °C/min. They reported that anorthite synthesis was achieved below 1000°C by the PVA steric entrapment route. The PVA content and its molecular length which had influenced the cation distribution, affected the powder morphology and the crystallization behavior. In addition to the contribution of polymer for low temperature synthesis of anorthite, the planetary milling also promoted the decrease in crystallization temperature by the exerted stresses (Lee and Kim 2002).

Traoré et al., studied the gehlenite and anorthite crystallization from kaolinite and calcite mixtures. All raw materials were wet ground (90 wt% < 8 µm) for 1 hour in an alumina jar with alumina balls. The powders die pressed and sintered at 1100°C for 1 hour with a heating rate of 3°C/min. They stated that first reaction was formation of gehlenite intermediate phase and calcium compounds from metakaolinite and calcium.



The second reaction was the anorthite crystallization from gehlenite, remaining alumina and quartz.



They concluded that the preferential reaction sequence was metakaolinite – gehlenite – anorthite due to the structural similarities of these layered structures (Traoré et al. 2003).

Also, Okada et al., investigated the effects of grinding and firing conditions on anorthite formation by solid state reaction of kaolinite with calcium carbonate. The appropriate amounts of kaolinite and  $\text{CaCO}_3$  mixed and ground at 300 rpm for 1 hour to 24 hours in alumina jar with alumina balls. The ground mixtures fired at various temperatures (500-1000°C) for 24 hours with a heating rate of 10°C/min. They concluded that grinding treatment was effective in reducing the particle size of the mixture. Grinding also activated the particles, accelerated the dehydroxylation of the kaolinite, and promoted decomposition of  $\text{CaCO}_3$ . The effect of grinding treatment on crystallization temperature had little influence. However, the grinding had influence on the crystallized products. Such that, the main phase in unground sample was gehlenite. But, the main phase in ground sample was layered  $\text{CaAl}_2\text{SiO}_8$  at the same firing conditions. Single anorthite phase was produced at 1000 °C with soak time of 12 hours (Okada et al. 2003).

Boudchicha et al., studied the crystallization of cordierite and anorthite based binary ceramics. The raw materials used in this study were kaolinite ( $\text{Al}_2\text{O}_3 \cdot 2\text{SiO}_2 \cdot 2\text{H}_2\text{O}$ ) and dolomite ( $\text{CaO} \cdot \text{MgO}$ ). The raw materials mixed in aqueous media then heat treated at 1250 °C for 3 hours. Next, calcined product was ball milled and compacted. The sintering of the compacts were done at a temperature range between 1200°C and 1350°C for 1 hour. As a conclusion, they reported that dense anorthite and cordierite based binary ceramics can be produced at 1350°C without employing complicated glass and sol-gel routes (Boudchicha 2001).

In a more recent study, Guechi et al., investigated the effect of temperature and  $\text{Na}_2\text{CO}_3$  addition on anorthite crystallization. They used local limestone and kaolin as raw materials. The raw materials mixed in appropriate amount, wet ball milled for 17 hours. Then the mixture was dried and calcined at 800°C for 2 hours.  $\text{Na}_2\text{CO}_3$  was added in the range of 0.5-3 wt%. Afterwards, the mixtures again wet ball milled for 4 hours with a proceeding drying at 150°C. Then, the mixtures in powder form were uniaxially pressed at 250 MPa and fired at temperatures between 750°C to 1100°C for 1 hour at a heating rate of 6°C/min. As a result, they reported that 96% theoretical density

was obtained from local raw materials with mechanical activation and without  $\text{Na}_2\text{CO}_3$  addition which sintered at  $900^\circ\text{C}$  for 1 hour. Further increase in relative density was achieved (97% theoretical density) both employing mechanical activation and 0.5 wt%  $\text{Na}_2\text{CO}_3$  addition which sintered at  $850^\circ\text{C}$  for 1 hour (Guechi et al. 2004).

Kobayashi and Kato studied low temperature fabrication of anorthite ceramics. For this purpose they employed excessive grinding for controlling the particle size of calcite which was one of the raw materials used for anorthite synthesis in this study. The other raw materials used for anorthite synthesis was New Zealand kaolin. The mean particle size for calcite reduced up to  $1.5\ \mu\text{m}$  with addition of ethanol in high alumina mills. The kaolin and fine calcite mixed and was ultrasonically dispersed in 200 ml deionized water for 20 minutes. The dried powder mixture was uniaxially pressed at 50 MPa to form pellets. The pellets were fired at  $1000^\circ\text{C}$  with a heating rate of  $400^\circ\text{C}/\text{h}$  in air. Above  $1000^\circ\text{C}$ , heating rate was decreased to  $200^\circ\text{C}/\text{h}$ . The soaking time was fixed at 1 hour. As a result of their study, they stated that decrease in particle size of calcite increased the density of fired products. They also stated that there was a significant density increase with increase in sintering temperature from  $900^\circ\text{C}$  to  $950^\circ\text{C}$ . Nevertheless, there was no significant density increase with the increase in sintering temperature from  $950^\circ\text{C}$  to  $1200^\circ\text{C}$  (Kobayashi and Kato 1994).

### **2.2.2. The CaO- $\text{Al}_2\text{O}_3$ - $\text{SiO}_2$ System**

Ternary phase diagram of CaO- $\text{Al}_2\text{O}_3$ - $\text{SiO}_2$ , which is illustrated in Fig 2.3., is important for understanding the behavior of anorthite ceramics. There are several binary compounds in CaO- $\text{Al}_2\text{O}_3$ - $\text{SiO}_2$  system such that Mullite ( $3\text{Al}_2\text{O}_3 \cdot 2\text{SiO}_2$ ), Wollastonite ( $\text{CaO} \cdot \text{SiO}_2$ ) and Grossite ( $\text{CaO} \cdot 2\text{Al}_2\text{O}_3$ ). The ternary compounds of the CaO- $\text{Al}_2\text{O}_3$ - $\text{SiO}_2$  system are Gehlenite ( $2\text{CaO} \cdot \text{Al}_2\text{O}_3 \cdot \text{SiO}_2$ ) and Anorthite ( $\text{CaO} \cdot \text{Al}_2\text{O}_3 \cdot 2\text{SiO}_2$ ). Relatively low liquidus and solidus temperatures prevail, inspite of the high melting temperatures of the three end members Pure  $\text{SiO}_2$  melts at  $1723^\circ\text{C}$ . The approximate melting temperatures for CaO and  $\text{Al}_2\text{O}_3$  are  $2570^\circ\text{C}$  and  $2020^\circ\text{C}$  respectively. Very little mutual solubility exists among the crystalline phases, because the ions  $\text{Ca}^{+2}$ ,  $\text{Al}^{+3}$  and  $\text{Si}^{+4}$  are sufficiently different in size to prevent extensive substitution of one ion for another in the crystal lattices (Muan A. and Osborn E. F. 1964).

Anorthite crystallization region is positioned in the middle of the ternary phase diagram and anorthite region is surrounded by mullite, tridymite, alumina, gehlenite and  $\alpha$ -calcium silicate. The stoichiometric anorthite has chemical composition of 20.16 wt% CaO, 36.66 wt%  $\text{Al}_2\text{O}_3$ , and 43.19 wt%  $\text{SiO}_2$ . According to the phase diagram in Figure 2.2. the congruent melting temperature for anorthite is  $1553^\circ\text{C}$  (Gdula 1971). Congruent melting means that solid compound of anorthite melts to form liquid of its own composition.

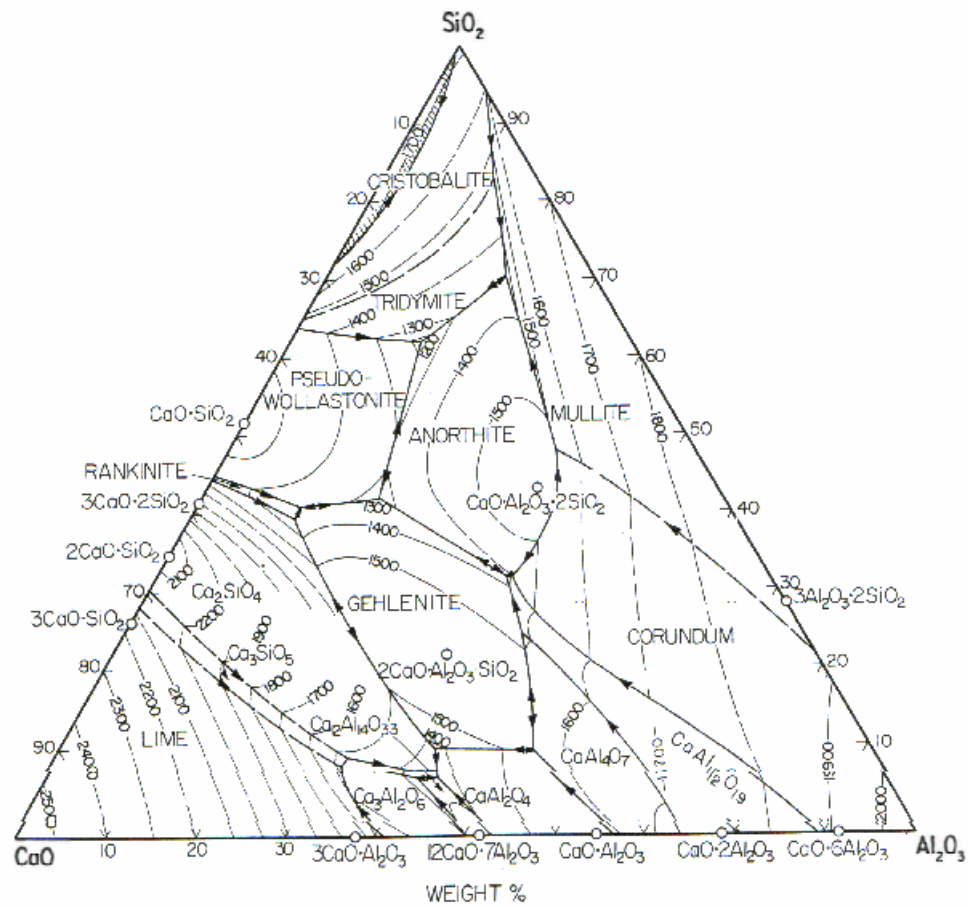


Figure 2.3.  $\text{CaO-Al}_2\text{O}_3\text{-SiO}_2$  Ternary Phase Diagram  
(Source: Rankin and Wright, 1915, Greig, 1927)

## CHAPTER 3

### EXPERIMENTAL

#### 3.1. Materials

Raw materials used for anorthite synthesis were Sivas Kaolin, ACS reagent calcium carbonate ( $\text{CaCO}_3$ ) (Sigma, ALDRICH) reagent grade aluminium hydroxide (Gibbsite) ( $\text{Al}(\text{OH})_3$ ) (MERCK) and calcined reactive alumina ( $\text{Al}_2\text{O}_3$ ) (ALCOA CT3000SG).

**Sivas Kaolin** ( $\text{Al}_2\text{O}_3 \cdot 2\text{SiO}_2 \cdot 2\text{H}_2\text{O}$ ): Kaolin is the most common starting mineral in the production of anorthite (Gdula 1971, Mergen and Aslanoğlu 2003, Mergen et al. 2004, Kobayashi and Kato 1994, Boudchicha 2001, Guechi 2004, Okada et al. 2003, Traoré et al. 2003). It is used as a source of  $\text{SiO}_2$  and  $\text{Al}_2\text{O}_3$ . In addition, it provides plasticity to the batch and helps maintain the shape and strength of the body during drying and firing (Çakır 1981). Kaolin also fuses over a temperature range depending on the composition which results in dense and strong bodies without buckling or losing shape at relatively lower temperatures (Kingery 1975). Sivas kaolin was recently studied for its composition and mineralogical characteristics. It was found that Sivas kaolin has low impurity content (Kırıkoğlu et al. 2004). XRD (X-Ray Diffraction) analysis of Sivas kaolin showed that it was composed of kaolinite (JCPDS card: 06-0221) with some quartz (JCPDS card: 86-1629) as shown in Figure 3.1. So, Sivas kaolin was chosen as a raw material in this study because of its low impurity content, low price and also it is easily available. Although Sivas kaolin is a low impurity clay, it cannot meet the perfect stoichiometry of the kaolinite mineral because the naturally occurring material also contains other impurity minerals like quartz. But quartz is not a problem constituent because it is also needed in the synthesis of anorthite.

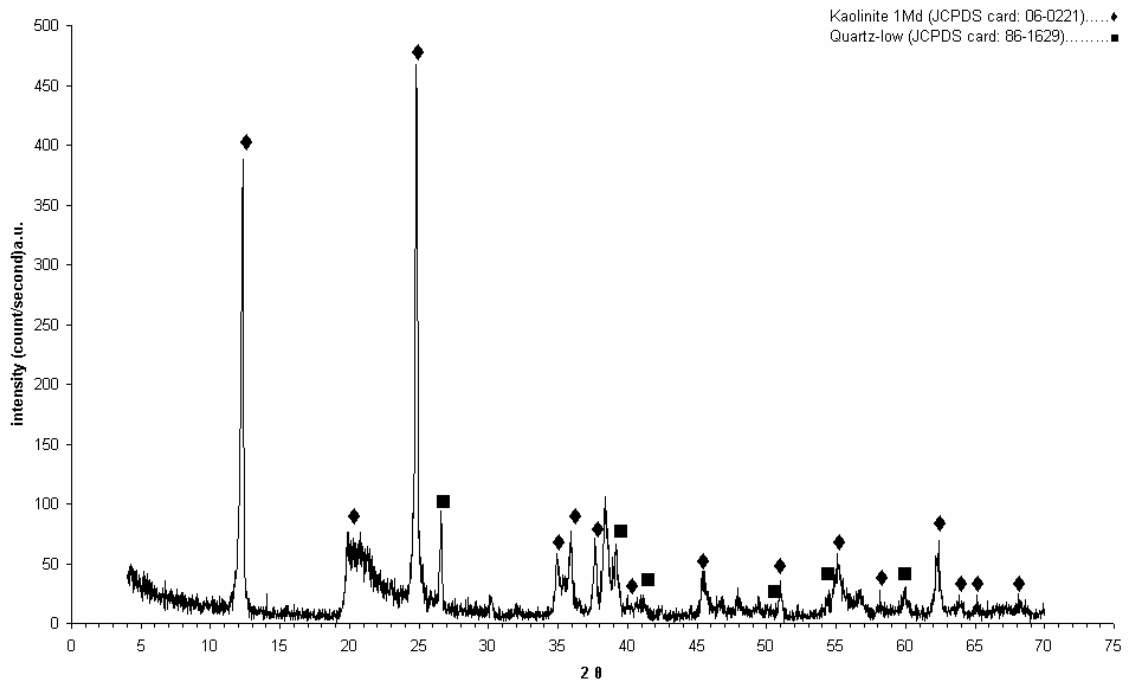


Figure 3.1. XRD analysis of raw material Sivas Kaolin (CuK $\alpha$  radiation was used).

**Calcined reactive (Superground) Alumina ( $\text{Al}_2\text{O}_3$ ) (ALCOA CT3000SG):** It is a common material that is used in electronics industry as a dielectric substrate material. In this study, alumina was used as the source of alumina to complement alumina deficiency of Sivas kaolin to match the stoichiometry (Çakır 1981).

**Aluminium Hydroxide:** Another material that was used as a source of  $\text{Al}_2\text{O}_3$  in anorthite synthesis was reagent grade aluminium hydroxide (Gibbsite) ( $\text{Al}(\text{OH})_3$ ) (MERCK).

**Calcium Carbonate ( $\text{CaCO}_3$ ):** In this study, calcium carbonate was used as a source of CaO for anorthite synthesis. It is one of the main raw materials used in anorthite synthesis in many studies (Gdula 1971, Mergen and Aslanoğlu 2003, Mergen et al. 2004, Kobayashi and Kato 1994, Okada et al. 2003, Traoré et al. 2003).

**Colemanite ( $2\text{CaO} \cdot 3\text{B}_2\text{O}_3 \cdot 5\text{H}_2\text{O}$ ):** Colemanite is a boron containing compound used as additive for decreasing the synthesis temperature of anorthite. It was obtained from Eti Holding A.Ş. Colemanite was added to stoichiometric mixture between 1 to 5 wt%. Influence of colemanite addition on the sintering behavior of anorthite has been recently studied (Mergen et. al. 2004). Boron containing additives were selected in this study due to the low melting point ( $450^\circ\text{C}$ ) of  $\text{B}_2\text{O}_3$  (Bergeron and Risbud 1984) and

due to less negative effect on insulating characteristics than the other sintering aids.

**Boric acid ( $H_3BO_3$ ):** Boric acid is another boron containing sintering aid used in this study because of the same reasons as colemanite and also obtained from Eti Holding A.Ş. Addition of boric acid ( $H_3BO_3$ ) for anorthite synthesis was also recently studied (Mergen and Aslanoğlu 2003). The chemical analyses of the raw materials used in anorthite synthesis is given in Table 3.1. The physical properties of raw materials are shown in Table 3.2.

Table 3.1. Chemical analyses of the raw materials and additives  
(Kırıkoğlu et al. 2004, Alcoa 2001).

	<b>Sivas Kaolin</b>	<b>CT3000SG Alumina (ALCOA)</b>	<b>Colemanite (Eti Holding)</b>	<b>BoricAcid (Eti Holding)</b>
$Al_2O_3$	33.07	99.6	0.00	0.00
$SiO_2$	52.86	0.03	6.5	0.00
$MgO$	0.00	0.09	0.00	0.00
$Na_2O$	0.13	0.08	0.00	0.00
$K_2O$	0.12	0.00	0.00	0.00
$CaO$	0.47	0.02	27	0.00
$Fe_2O_3$	0.05	0.02	0.00	0.00
$TiO_2$	0.38	0.00	0.00	0.00
$MnO$	0.10	0.00	0.00	0.00
$SO_3$	0.60	0.00	0.00	0.00
$B_2O_3$	0.00	0.00	42.50	56.25
LOI	12.22	0.16	-	-
Total	100.00	100.00	100.00	100.00

Table 3.2. Physical properties of as-received raw materials and additives  
(Kırıkoğlu et al. 2004, Alcoa 2001).

	<b>CaCO<sub>3</sub></b> (Aldrich)	<b>Sivas</b> <b>Kaolin</b>	<b>CT3000SGA</b> <b>lumina</b> (ALCOA)	<b>Aluminium</b> <b>Hydroxide</b> (Al(OH) <sub>3</sub> )	<b>Colmanite</b> (Eti Holding)	<b>BoricAcid</b> (Eti Holding)
<b>Density</b> (g/cm <sup>3</sup> )	2.93	2.62	3.9	2.42	-	1.44
<b>Molecular</b> <b>Weight</b>	100.09	258.16	102	77.99	-	61.83
<b>Particle size</b> (µm)	-	< 38	d <sub>mean</sub> =0.85	-	< 45	80

## 3.2. Method

### 3.2.1. Powder Mixture Preparation

The raw materials were mixed in proper amounts to obtain a 1:1:2 stoichiometric anorthite mixture. The amounts of raw materials and additives are tabulated in Table 3.3. In the first set of experiments only one source of Al<sub>2</sub>O<sub>3</sub> was used for each mixture: calcined alumina. At the later stages of the project aluminium hydroxide was also employed. Then, this mixture was wet milled (in 60 ml deionized water) in planetary mono mill. The grinding speed and time changed in range of 100-500 rpm, 15-75 min respectively. The ground slurry was spread on tray and dried at 103°C in electric oven. The agglomerates of particles were crushed with porcelain mortar and pestle to obtain fine powder. The powder was pressed uniaxially in universal hydraulic press to form pellets which were sintered in a global benchtop kiln at temperature range of 900°C - 1100°C with soaking time of 1 hour to 5 hours with constant heating rate of 10°C/min. The experimental procedure is schematically represented in Figure 3.2.

Table 3.3. The amounts of raw materials and additives for mixtures

Raw Material	Chemical Formula	Amount in grams
Sivas kaolin	$\text{Al}_2\text{O}_3 \cdot 2\text{SiO}_2 \cdot 2\text{H}_2\text{O}$	15g
Calcium Carbonate	$\text{CaCO}_3$	6.48g
Alumina	$\text{Al}_2\text{O}_3$	1.76g
Aluminium Hydroxide	$\text{Al}(\text{OH})_3$	2.692g
Colemanite	$2\text{CaO} \cdot 3\text{B}_2\text{O}_3 \cdot 5\text{H}_2\text{O}$	1 wt%-----0.540g
		3 wt%-----1.620g
		5 wt%-----2.760g
Boric Acid	$\text{H}_3\text{BO}_3$	1 wt%-----0.412g
		3 wt%-----1.236g
		5 wt%-----2.060g

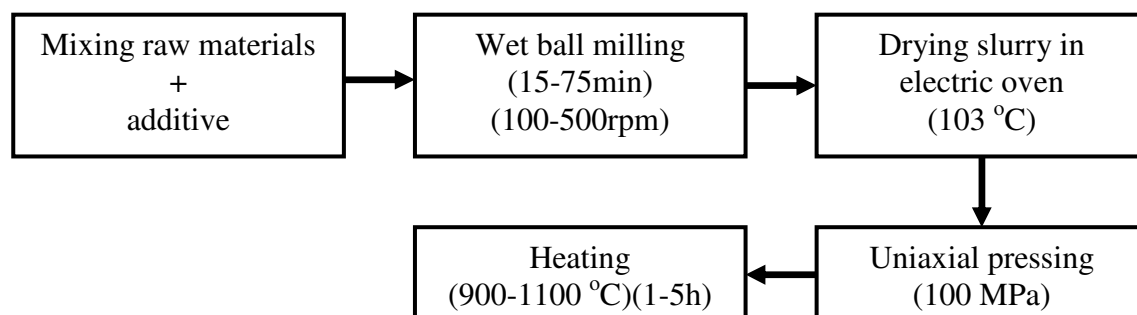


Figure 3.2. Schematic flow chart showing the main steps of sample preparation

### 3.2.2. Grinding

Mixtures were mechanically activated in a planetary mono mill (Fritsch Pulverisette 6), which is represented in Figure 3.3. Thirty tungsten carbide balls each with a diameter of 10 mm were used as the grinding media in a 250 ml tungsten carbide pot. The grinding speed and time were varied from 100 to 500 rpm and 15 to 75 min, respectively.

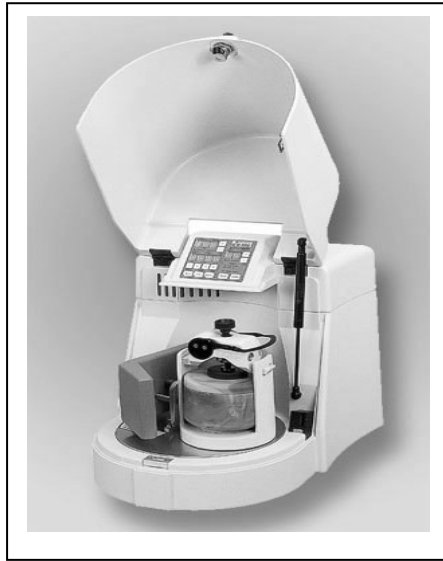


Figure 3.3. Planetary mono mill.

### **3.2.3. Compaction**

The powders were pressed uniaxially in a universal hydraulic press (Yıldız Hidrolik San.Tic,2001 Model) at 100 MPa pressure in a stainless steel die to form pellets.

### **3.2.4. Heat Treatment**

The compacted pellets for anorthite synthesis were heated in a 5 liter (Figure 3.4) globar benchtop kiln (Alser Teknik A.Ş. Protherm PLF 160/5) which used an “S” type thermocouple for temperature measurement. The heating (sintering) for anorthite synthesis was done in a temperature range of 900°C - 1100°C with soaking time of 1 hour to 5 hours with constant heating of 10°C/min. The kiln was allowed to cool by itself in air.



Figure 3.4. Global benchtop kiln.

### 3.3. Product Analysis

#### 3.3.1. X-Ray Diffraction Analyses

X-ray diffraction (XRD) with Cu K $\alpha$  radiation with wavelength  $\lambda=1.54$  Å, was used to detect the present phases and crystallinity of the ground and heated mixtures (Philips X'pert Pro, XRD).

X-ray intensity was determined by the diffraction peak heights using the position listed in Table 4.6. Philips X'Pert Graphics & Identify program was used for X-ray diffraction analyses. The JCPDS card number and peak positions used for XRD peak intensity measurements are given in Table 3.4.

Table 3.4. JCPDS card number and peak positions used for XRD peak intensity measurements.

Mineral	JCPDS number	(hkl)	Diffraction angle ( $2\theta$ )
Anorthite	41-1486	(004)	28.03°

### **3.3.2. Microstructural Analyses (SEM)**

The morphology and particle size of the mixtures were observed by scanning electron microscope (Philips XL-30S FEG, SEM).

### **3.3.3. Density and Porosity Measurements**

The density and porosity of the synthesized pellets of anorthite mixtures were determined using Archimedes' technique. (ASTM C 20-87) (ASTM 1987). This testing method enables the determination of apparent porosity, water absorption, and bulk density of the anorthite mixtures. A balance with Archimedes' apparatus (Precisa-XP220A) was used for the measurement of density and porosity values.

## **3.4. Statistical Experimental Design**

Statistical experimental design can increase the efficiency of experiments. In this study, two-level and three level fractional factorial design models were selected. The key in statistical experiment design is that it enables the researcher to obtain maximum possible amount of information from a limited number of experiments. The  $2^k$  design is particularly useful in the early stages of experimental work, when there are likely to be many factors to be investigated. It provides the smallest number of runs with which  $k$  factors can be studied in a complete fractional factorial design. Consequently, these designs are widely used in factor screening experiments (Montgomery 2005).

In this study, the following experimental design methodology was employed. First, a pool of important factor effects was formed and those factors that can be controlled within the experimental apparatus were chosen. This group of factors contained six parameters which were reduced to the more important three parameters as a result of the Plackett-Burman screening experiment set. The remaining three parameters were more closely investigated via the use of a Box-Behnken response surface experiment set. This time each factor was studied at three different levels as opposed to the two levels used in the previous screening experiment set. Finally, ladder

experiments were conducted to more closely understand the effect of the most important parameters.

### 3.4.1. Fractional Factorial Design

As the number of factors in a  $2^k$  factorial design increases, the number of runs required for a complete replicate of the design geometrically increases. For example, a complete replicate of  $2^6$  design requires 64 runs. In this design only 6 of the 63 degrees of freedom correspond to main effects, and only 15 degrees of freedom correspond to two factor interactions. The rest of degree of freedoms are associated with three or higher effect interactions. Degree of freedom allocation for  $2^6$  design is presented in Table 3.5 for the main factors and their interactions. If the experimenter can reasonably assume that certain high order interactions are negligible, then instead of running all the experiments, a fraction of the complete factorial experiments can be run for obtaining main effects and low-order interactions. These fractional factorial designs are among the most widely used types of statistical designs for product and process designs and for process improvement.

Table 3.5. Distribution of degree of freedoms for  $2^6$  design

Source of Variation	Degrees of Freedom
$2^6$ design	63
Main Effects	6
2 factor interactions	15
3 factor and higher order interactions	42

The fractional factorial design is based on three principles. These principles are sparsity of effects principle, projection property and sequential experimentation.

**The sparsity of effects principle:** If there are several factors or variables that affect the process or system, the system or process is likely to be driven primarily by

some of the main effects and low order interactions. In other words, higher interactions of variables have negligible affect on the process or system.

**The projection property:** Fractional factorial designs can be projected into larger (stronger) designs in the subset of significant factors.

**Sequential experimentation:** The runs of two or more fractional factorial designs can be combined to assemble a larger design to estimate factor effects and interactions of interest.

### 3.4.1.1. Plackett- Burman Screening Design

A major use of fractional factorials is in screening experiments. These are experiments in which the more important factor effects are identified in the early stages of a project when it is likely that many of the factors initially considered have little or no effect on the response. The factors that are identified as important are reinvestigated in subsequent experiments (Montgomery 2005). They allow the experimenter to evaluate large number of experimental factors with very few numbers of experiments and without the need to replicate experiments to draw statistically valid conclusions (Leigh and Towe 1987).

Plackett-Burman Screening Design is proposed by R.L.Plackett and J.P. Burman in 1946. It is a specific fraction of 2 level factorial design ( $2^k$ ) that has properties that allow efficient estimation of the effects of the variables under study (Harris and Lautenberger 1976). These design were performed with  $k=N-1$  factors. N is the number of runs, where N is a multiple of 4. These designs are similar to fractional factorial designs, except the designs with  $N=12, 20, 24, 28$  and  $36$  which can not represented as cubes and they are often called nongeometric designs.

Table 3.6. shows the number of factors (k), required runs (N) and their plus (high level of each factor) and minus(low level of each factor) signs for their first rows. The other rows are generated from these first rows. Such that, second row is generated the by moving of the elements of first row one position to the right and then placing the last element of the first row to the first place in the second row. This proceeds until all the rows are generated except the last row which is composed of only minus signs. So, the plus and minus signs follows diagonal in the each row except the last row. The design for  $N=12$  runs and  $k=11$  factors is shown in Table 3.7

Table 3.6. Plus and minus signs for first rows of the Plackett-Burman designs

k =11	N =12	+ + - + + + - - - + -
k =19	N =20	+ + - - + + + + - + - + - - - + + -
k =23	N =24	+ + + + + - + - + + - - + + - - - + - - - -
k =35	N =36	- + - + + + - - - + + + + - + + + - - + - - - - + - + - + + - - + -

Plackett-Burman design is a powerful technique that can handle the estimates of main factor effects clear of each other. However, they are not capable of identifying significant interactions. It is recommended that, Plackett-Burman designs are used up to seven factors for 12-run designs, 15 factors for the 20-run designs and 23 factors for the 28-run design. This makes it possible to estimate the experimental error from the design data. Because the remaining “unassigned” columns provide the error estimate during analysis of the data. In our design, there are 5 columns dedicated to unassigned factor effects (represented in Table 3.7.) Columns from G to L are used as experimental error estimators. The plus and minus signs indicate high and low levels of independent variables.

Table 3.7. Design set of experiments for Plackett-Burman design with 12 runs.

Run Order	Mixtures	Factors										
		Variables						Unassigned columns				
		A	B	C	D	E	F	G	H	J	K	L
5	S9	+	+	-	+	+	+	-	-	-	+	-
7	S12	+	-	+	+	+	-	-	-	+	-	+
11	S10	-	+	+	+	-	-	-	+	-	+	+
9	S5	+	+	+	-	-	-	+	-	+	+	-
4	S1	+	+	-	-	-	+	-	+	+	-	+
1	S11	+	-	-	-	+	-	+	+	-	+	+
2	S4	-	-	-	+	-	+	+	-	+	+	+
12	S6	-	-	+	-	+	+	-	+	+	+	-
3	S8	-	+	-	+	+	-	+	+	+	-	-
8	S3	+	-	+	+	-	+	+	+	-	-	-
10	S7	-	+	+	-	+	+	+	-	-	-	+
6	S2	-	-	-	-	-	-	-	-	-	-	-

In our study, we had five continuous variables; additive amount(B), sintering temperature(C), soaking time(D), grinding time(D), grinding speed(F) and one discrete variable of additive type(A). High and low levels for these variables are shown in Table 3.8.

Table 3.8. The factors for Plackett-Burman screening design

Factor	<i>k</i>	High level (+)	Low level (-)	Type of variable
Additive type	A	Boric acid	Colemanite	discrete
Additive amount	B	5 wt%	1 wt %	continuous
Sintering temperature	C	1100 °C	900 °C	continuous
Soaking time	D	5 hours	1 hour	continuous
Grinding time	E	60 min.	15 min.	continuous
Grinding speed	F	500 rpm	100 rpm	continuous

The values for the response variable were measured from the main peak intensities of anorthite from XRD patterns. For response, the height of the strongest X-ray peak for anorthite was selected. According to JCPDS card number 41-1486, strongest peak of anorthite is positioned at  $2\theta$  value of  $28.03^\circ$ .

### 3.4.1.2. Response Surface Design

Describing the relation of one or more dependent variables to several independent variables in a process or system can be expressed by mathematical equations or models. Models can be theoretical or empirical. However, in most processes or systems the exact theoretical model is rarely known. So, generally empirical models have been used to approximate the response according to process data. A general system or process has inputs and one or more outputs. So, mathematical expression can be expressed as follows:

$$y_1 = f_1(x_1, x_2, \dots, x_n)$$

$$y_2 = f_1(x_1, x_2, \dots, x_n)$$

•

•

•

$$y_m = f_1(x_1, x_2, \dots, x_n)$$

Response surface designs are powerful tools for obtaining 2<sup>nd</sup> order polynomial approximations with their quadratic terms. The mathematical expression for a response surface design with n independent variables:

$$y = b_0 + \sum_{i=1}^n b_i x_i + \sum_{i=1}^n b_{ii} x_i^2 + \sum \sum_{i < j} b_{ij} x_i x_j \dots \dots \quad (3.1)$$

Response surfaces obtained for a particular process or system by running experiments in the independent variables and observing the response variables. These response observations are used to estimate the coefficients for the mathematical expression above. Response surfaces are very powerful in estimating the responses for dependent variables over the range that they generated. However they do not work well when they are used for extrapolation from the region that are employed. A desirable response surface design should have the following properties:

- Provide a reasonable distribution of data points and information over the range of interest
  - Allow model adequacy
  - Allow to run experiments in blocks
  - Allow to build higher order designs sequentially
  - Provide an internal estimate of error
  - Estimates for model coefficients should be precise in the experimental region
  - Provide reasonable estimates for the prediction variance in the experimental region
- Should be robust against outliers and missing values
- Does not require large number of runs
- Does not require too many levels for independent (input) variables

- Ensures simplicity of calculation of the model parameters.

The required number of runs for generating response surface design is given in Table 3.9 for various number of factors. Second column shows the number of trials for three level full factorial design and the last column shows the required number of coefficients in the full quadratic polynomial model which is also the minimum number of data points required for response surface design. Any response surface design must have more data points than these minimum values to provide degrees of freedom from which an estimate for the error variance can be obtained.

Table 3.9. Required number of runs in three level factorial designs

Number of Independent Variables (Factors)	Number of Trials in Full Three Level Factorial	Number of Coefficients in Full Quadratic
2	9	6
3	27	10
4	81	15
5	243	21
6	729	28

Box-Behnken Design: These designs attributed to G. E. P. Box and D. W. Behnken in 1960. Box- Behnken design employs subset of the points in the corresponding full-three level factorial. For example, a Box- Behnken design requires 15 run points in which 3 run points are at the center of the design cube. A three level, three factorial design requires 27 run points. However, Box-Behnken design requires 15 run points for three factors. The extra five points for Box Behnken design then the minimum required value for full quadratic model, which is shown in Table 3.9. provides 5 degrees of freedom for error. So, Box- Behnken designs are very efficient in terms of required number of runs and they are rotatable or nearly rotatable. Rotability means that the response surface design should provide equal precision of estimation independent of the direction.

The geometric shape for Box- Behnken design is shown in Figure 3.5. All the points positioned at the middle of the edges of the cube except for the 3 center points. The run (data) points tabulated in Table 3.10 according to the coded levels for the

independent variables (factors). The plus one indicates high level, zero indicates middle level and minus one indicates low level for that independent variable. Infact, the Box-Behnken design is not cuboidal. Box- Behnken design is a spherical design that all data points on edges of the cube also lie on the surface of a sphere and have equal distances from the center which is  $\sqrt{2}$  times the corner length of the cube. The replicated data points in the center of the sphere provide a measure of inherent experimental error and enable a relatively constant prediction of variance as a function of distance from the center. Also, Box- Behnken design structure for three factors is made up of three  $2^2$  design, each with one variable at the middle shown in Figure 3.6.

The values for the response variable were measured from the main peak intensities of anorthite from XRD patterns. For response, the height of the strongest X-ray peak for anorthite was selected. According to JCPDS card number 41-1486, strongest peak of anorthite is positioned at  $2\theta$  value of  $28.03^\circ$ . The results of the design were analyzed with commercial software named Design-Expert 7.0.

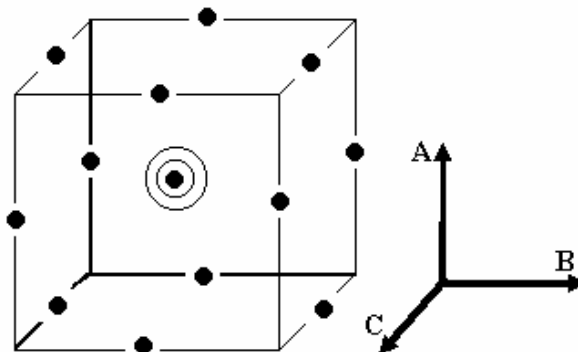


Figure 3.5. Box-Behnken design for three factors

Table 3.10. The coded levels of independent variables for three variable Box-Behnken design

Run Order	Variable A	Variable B	Variable C
1	+	+	0
2	+	-	0
3	-	+	0
4	-	-	0
5	+	0	+
6	+	0	-
7	-	0	+
8	-	0	-
9	0	+	+
10	0	+	-
11	0	-	+
12	0	-	-
13	0	0	0
14	0	0	0
15	0	0	0

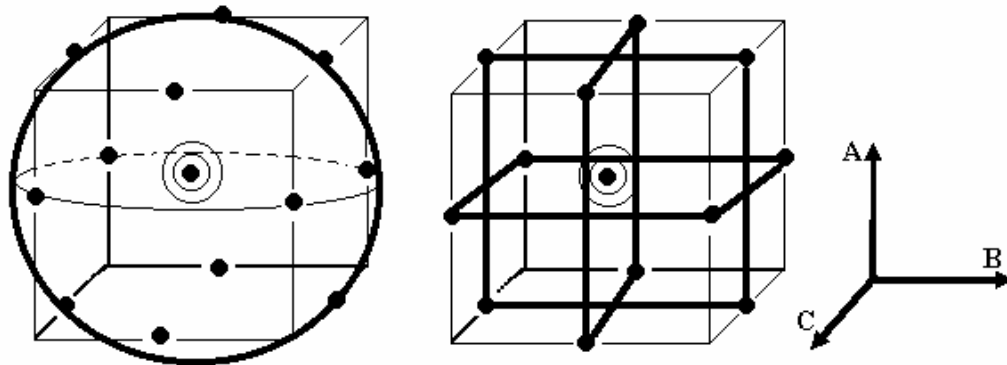


Figure 3.6. Geometrical structure of Box-Behnken design for three factors

## CHAPTER 4

### RESULTS AND DISCUSSION

#### 4.1. Anorthite Synthesis

As explained in detail in Chapter 3, mixtures were prepared by mixing raw materials in proper amounts and were ground for 15 minutes to 75 minutes each time at different grinding speeds that varied from 100 rpm to 500 rpm in a planetary mono mill. After uniaxial compaction, the samples were fired in the kiln at high temperatures. The sintering temperature varied from 800 °C to 1100 °C. and soak time were changed from 1 hour to 5 hours. Two different boron containing additives were used in order to investigate their effects on anorthite phase formation. Finally, the effect of the source of alumina as a starting raw material was studied to investigate its effect on anorthite formation.

##### 4.1.1. Labeling System Used for Samples in Anorthite Synthesis

A labeling system was used in the following sections, because of the large number of samples that were studied. There were a total of six parameters that were studied and the coding is shown below:

- 1) Additive type (Colemanite (C)-Boric Acid (B)),
- 2) Additive amount (1-5 wt%),
- 3) Sintering temperature (800-1300°C),
- 4) Soak time during heating (1-5 hrs),
- 5) Grinding duration (15-75 minutes),
- 6) Grinding rotational speed (100-500 rpm),

The samples were labeled with capital letters which denote the type of experimental set and the conditions respectively. Such that, S represents that it is a screening experiment, R represents that it is a response surface experiment, G represents it is a grinding effect experiment and A represents that it is an experiment in which Al(OH<sub>3</sub>) used as alumina source instead of Al<sub>2</sub>O<sub>3</sub>.

For example, the sample labeled as S3-C-1-1100-5-15-500 indicates that this sample is the 3<sup>rd</sup> sample in screening design set (Table 4.3.). This sample was prepared with addition of 1 wt % colemanite(C), it was sintered at 1100 °C for 5 hours. The mixture was wet milled in planetary mono mill for 15 minutes at 500 rpm.

#### **4.1.2. Results of Plackett-Burman Screening Design for Anorthite Synthesis**

In order to minimize the number of runs and to determine the more important factor effects screening design methodology was employed. Based on the variables listed in Table 3.8, the screening experiments were done according to the experimental points listed in Table 3.7. These parameters were additive type, additive amount, sintering temperature, soak time, grinding time and grinding rotational speed. The other experimental conditions were fixed for all samples. Such that, heating rate and cooling rate during firing was fixed to 10°C/min. The compaction of the powders was done at a pressure of 100 MPa. The grinding was carried in tungsten carbide jar with tungsten carbide balls having a diameter of 10 mm.

The XRD patterns for the Plackett-Burman screening design are shown in Figure 4.1. The main phase detected in samples that were fired at 1100 °C was anorthite with a small amount of corundum phase such as in sample S6-C-1-1100-1-60-500. On the contrary, samples that were heated at 900°C also contained other phases in addition to the anorthite phase except for sample S9-B-5-900-5-60-500 and S1-B-5-900-1-15-500. These other phases were gehlenite, quartz, calcium silicate and calcium borate. In samples, S11-B-1-900-1-60-100 and S2-C-1-900-1-15-100 the anorthite phase was not detected. The main phase in these samples was corundum with minor phases of gehlenite, calcium silicate, and quartz.

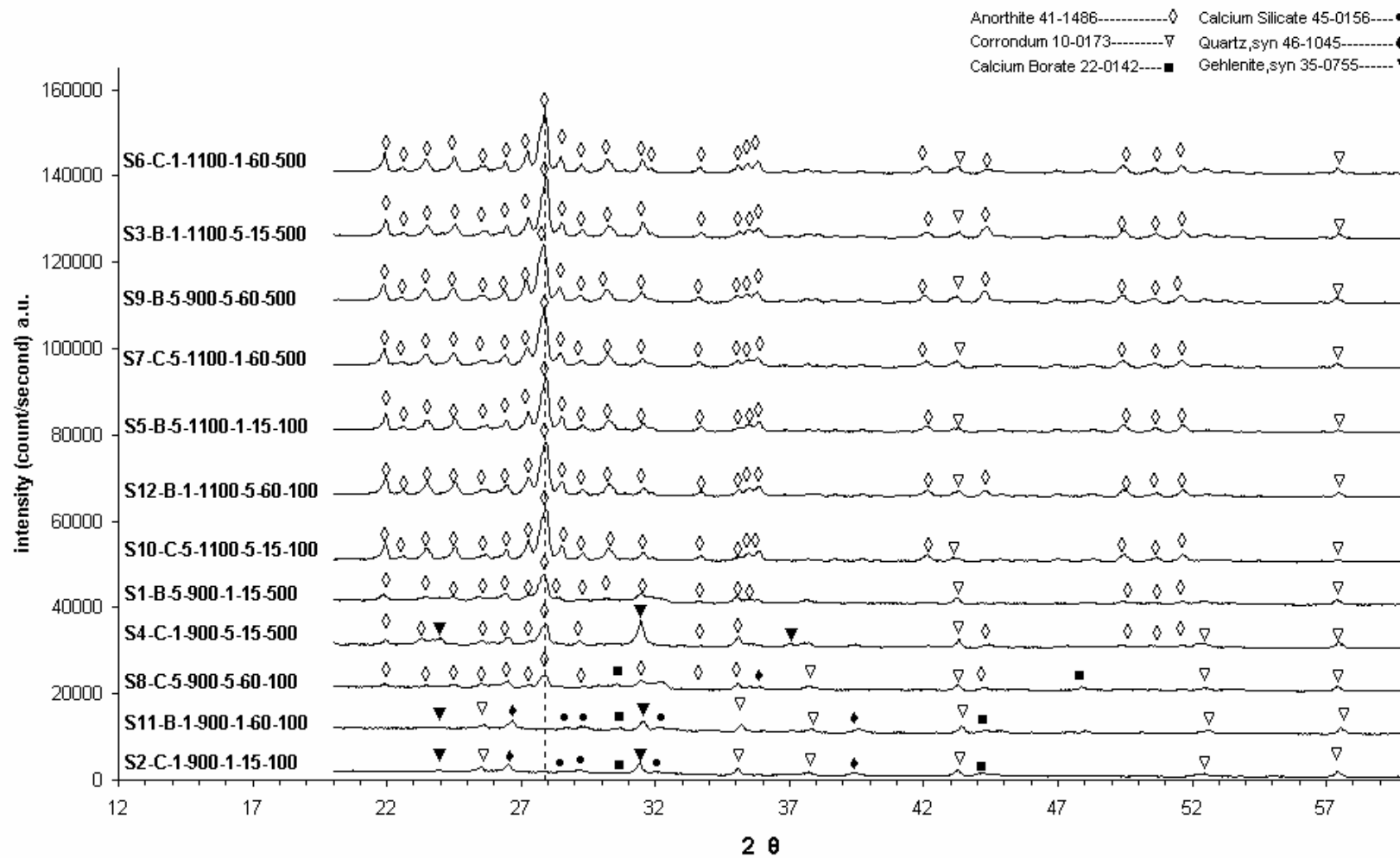


Figure 4.1. XRD patterns of the Plackett-Burmann screening design samples

The responses for Plackett-Burman screening design are tabulated in Table 4.1. The maximum response 1456 was observed in S6-C-1-1100-1-60-500 batch. In this batch, firstly 1 wt % of colemanite was added in the mixture then the mixture was ground at 500 rpm for 60 min before compaction for firing. The pellets were heated at 1100°C for 1 hour.

To find the main factors in our design, firstly, statistical computations were done by hand and results are shown in Table 4.1. (Harris and Lautenberger 1976) First, critical minimum difference [MIN] was calculated as shown in equation 4.1.

$$S_{FE} = \sqrt{\frac{1}{q} * (UFE_1^2 + UFE_2^2 + \dots + UFE_q^2)} \quad (4.1)$$

$$[MIN] = t * S_{FE}$$

q (Number of unassigned factor effects) = n-k-1,

n = number of runs (n = 12 for 12 run Plackett-Burman design)

k = number of factors (k = 6 because 6 factors were studied)

UFE = Unassigned factor effect

t =  $t_{dof,\alpha}$  ( dof = 5 because there were 5 unassigned factor effects) ( $\alpha$  = confidence level)

Critical minimum differences [MIN] were calculated by multiplying the different t-values for different confidence levels of 90 %, 95 % and 97.5 % at 5 degree of freedom with the  $S_{FE}$  value. The factor effects that have greater absolute value than this value are considered to be significant factor effects and the others are insignificant. Degree of freedom was the number of unassigned factor effects (q). At the 95 % confidence level, sintering temperature(C), grinding speed(F), additive amount(B) and soak time(D) were the more important factors in decreasing order of importance (Table 4.1.).

In addition to the hand calculation, Design Expert 7.0. software program was used to find the main factors. The Plackett-Burmann toolbox was selected and design matrix was generated for 11 factors 12 runs. The factor names, units, type, and actual low and high levels sections were filled. Factors were specified as numerical (continuous) or categorical (discrete). Unused factors were coded from G to L. After

that, alias structure window was approved. Response name and unit were entered in the next screen. Finally, the design was created.

Table 4.1. Evaluation of Plackett-Burmann design

Run Order	Batches	A Additive type	B Additive amount	C Sintering Temp.	D Soak Time	E Grinding time	F Grinding speed	G	H	J	K	L	Response
1	<b>S9</b>	+	+	-	+	+	+	-	-	-	+	-	1357
2	<b>S12</b>	+	-	+	+	+	-	-	-	+	-	+	1291
3	<b>S10</b>	-	+	+	+	-	-	-	+	-	+	+	1282
4	<b>S5</b>	+	+	+	-	-	-	+	-	+	+	-	1318
5	<b>S1</b>	+	+	-	-	-	+	-	+	+	-	+	750
6	<b>S11</b>	+	-	-	-	+	-	+	+	-	+	+	0
7	<b>S4</b>	-	-	-	+	-	+	+	-	+	+	+	632
8	<b>S6</b>	-	-	+	-	+	+	-	+	+	+	-	1456
9	<b>S8</b>	-	+	-	+	+	-	+	+	+	-	-	438
10	<b>S3</b>	+	-	+	+	-	+	+	+	-	-	-	1401
11	<b>S7</b>	-	+	+	-	+	+	+	-	-	-	+	1349
12	<b>S2</b>	-	-	-	-	-	-	-	-	-	-	-	0
Sum +		6120,44	6498,34	8100,05	6403,68	5893,83	6948,03	5140,12	5329,42	5888,34	6047,94	5306,69	
Sum -		-5159,04	-4781,14	-3179,43	-4875,8	-5385,65	-4331,45	-6139,36	-5950,06	-5391,14	-5231,54	-5972,79	
Over-all Sum		11279,48	11279,48	11279,48	11279,48	11279,48	11279,48	11279,48	11279,48	11279,48	11279,48	11279,48	
Difference		961,4	1717,2	4920,62	1527,88	508,18	2616,58	-999,24	-620,64	497,2	816,4	-666,1	
Effect		160	<b>286</b>	<b>820</b>	<b>254</b>	84	<b>436</b>	-166	-103	82	136	-111	
									S <sub>FE</sub> =	123,4			
t distribution		t <sub>5,0.1</sub>	1.476					MIN=	182	(90 % Confidence Level)			
		t <sub>5,0.05</sub>	2.015					MIN=	248	(95 % Confidence Level)			
		t <sub>5,0.025</sub>	2.571					MIN=	317	(97,5 % Confidence Level)			

The half-normal probability plot of these effects generated by Design Expert 7.0 software, is presented in Figure 4.2. These plots graphically determine the factor effects that are significant or insignificant. If a factor effect that is positioned away from the diagonal line, then it is a significant factor effect. If it is located near this diagonal line, then its effect on the response is statistically insignificant. The important effects that emerge from this analysis were the main effects of C (sintering temperature), F (grinding speed), B (additive amount) and D (soak time). The unused factors effects (from G to L) were insignificant. This meant that there was no aliased interaction between factor effects. The hand calculations done in Table 4.1. were, therefore, confirmed by the software computations because the same parameters were identified to be significant.

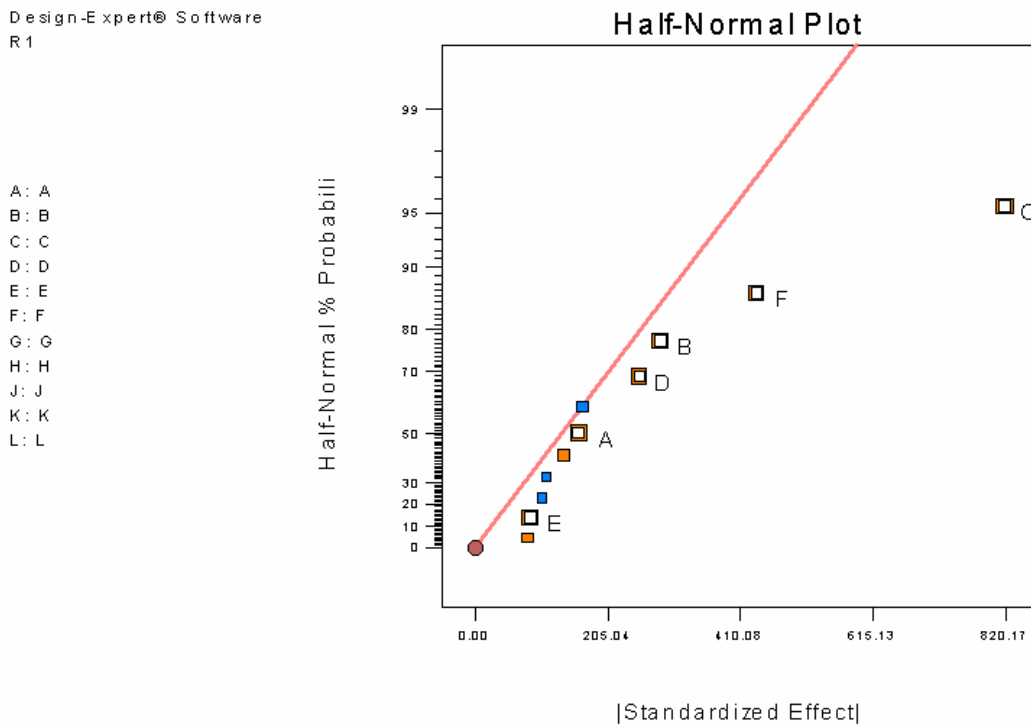


Figure 4.2. Half-Normal probability plot of the effects for the Plackett-Burmann design

The statistical analyses results (ANOVA table) for the screening experiments for anorthite synthesis are given in Table 4.2. The sum of squares was used as a measure of overall variability in the data. The value of 3.128E+006 indicates that the variation in the experiment data was very large. Mean square values were obtained by dividing the

sum of squares by the degrees of freedom. The model F-value of 11.42 implied that the model was significant. There was only a 0.86 % chance that a "Model F-Value" this large could occur due to noise. The significance of each term on the anorthite synthesis was shown by the values in column "Prob > F". Values of "Prob > F" less than 0.05 indicate that model terms were significant at the 95% confidence level. In other words we were 95% confident that the particular effect was significant. According to ANOVA table, C (sintering temperature) had the minimum Prob > F value and it was significant. Also, F (grinding speed) was a significant factor.

The Design Expert 7.0. software output for the Plackett-Burmann screening design is given in Table 4.3. The model R<sup>2</sup> value was 0.9320. That was about 93 percent of variability in the anorthite synthesis was explained by factor C (sintering temperature) and F (grinding speed). The "Pred R-Squared" of 0.6083 was not in close agreement with the "Adj R-Squared" of 0.8504. However, the Adeq Precision value was 10.241. This value measures the signal to noise ratio where, a ratio greater than 4 was desirable. So, the value of 10.241 indicated an adequate signal and this model can be used to navigate the design space.

Table 4.2. ANOVA table for the Plackett-Burmann screening design

Source	Sum of Squares	Degrees of freedom	Mean Square	F Value	p-value Prob > F	
Model	3.128E+006	6	5.213E+005	11.42	0.0086	significant
A	76960.08	1	76960.08	1.69	0.2508	
B	2.462E+005	1	2.462E+005	5.40	0.0678	Significant
C	2.018E+006	1	2.018E+006	44.22	0.0012	Significant
D	1.943E+005	1	1.943E+005	4.26	0.0940	
E	21420.75	1	21420.75	0.47	0.5238	Significant
F	5.707E+005	1	5.707E+005	12.50	0.0166	Significant
Residual	2.282E+005	5	45639.68			
Cor Total	3.356E+006	11				

Table 4.3. Design Expert 7.0. software output for the Plackett-Burmann screening design

Std. Dev.	213.63	R Squared	0.9320
Mean	939.92	Adj R Squared	0.8504
C.V. %	22.73	Pred R Squared	0.6083
PRESS	1.314E+006	Adeq Precision	10.241

### 4.1.3. Results of Box-Behnken Response Surface Design for Anorthite Synthesis

Box-Behnken response surface design was carried out in order to analyse the anorthite synthesis in the selected region and to maximize the anorthite synthesis. The more important factor effects that were selected by employing screening design were used as independent variables in Box-Behnken response surface design. These important factors screened in the previous section were sintering temperature(C), grinding speed(F), additive amount(B) and soak time(D). Because mechanochemical synthesis was more pronounced at high grinding speeds and the mill was only able to handle up to 500-600 rpms of continuous operation, this parameter was not further studied in the response surface sets of experiments. Grinding speed was held constant for all batches at 500 rpm. The effect of grinding time was selected as the additional parameter to study. The additive type parameter used in the screening design was selected as boric acid in order to maximize the anorthite phase formation. The soak time was fixed as 1 hour for all batches to reduce the time required for experimentation and to enable to run one experiment in one day. The other parameters like grinding media, compaction pressure, heating rate, etc. were all the same as they were in the screening design.

The response surface experiments were done according to the coded run points listed in Table 3.10. The actual levels of the factors are given in Table 4.4. Again, the response values measured from the length of the main peak intensities of anorthite from XRD patterns.

Table 4.4. The actual values of factors for Box-Behnken response surface design

Factor	<i>k</i>	Low level (-)	Middle level (0)	High level (+)	Type of variable
Sintering temperature	A	900 °C	1000 °C	1100 °C	continuous
Additive amount	B	1 wt %	3 wt %	5 wt%	continuous
Grinding time	C	15 minutes	45 minutes	75 minutes	continuous

The XRD patterns for the Box-Behnken response surface design are shown in Figure 4.3. and Figure 4.4. In all samples, the main phase was detected as anorthite with small amount of corundum phase. Also, gehlenite phase was detected in samples R4-B-1-900-1-45-500 and R8-B-3-900-1-15-500. Samples that were heated at 1100°C showed narrower and higher peaks of anorthite than the samples that were fired at lower temperatures. The height of peaks decreased and broadened with decreasing sintering temperature. Hence, the 900°C heat treatment was not fully sufficient for anorthite synthesis. At that temperature, the raw materials did not completely react with each other.

The responses for Box-Behnken response surface design are tabulated in Table 4.5. The maximum response of 1473 was observed in R6-B-3-1100-1-15-500 batch. Design Expert 7.0. software program was used for evaluation of the results and for generating the response surfaces for the factors listed in Table 4.4. This software is able to generate the response function with respect to the important factor effects. After generating the response surface, the optimum operation point that maximizes the response in the region was determined according to the response function.

The normal probability plot of the response surface design is presented in Figure 4.5. This plot indicates whether the residuals follow a normal distribution, in which case the points will follow a straight line. From the figure it can be concluded that the residuals are distributed normally. In addition, the center-point-replication runs in the Box-Behnken design were repeated one more time to confirm the reproducibility of data. The margin of variation was small and the experimental system was rugged.

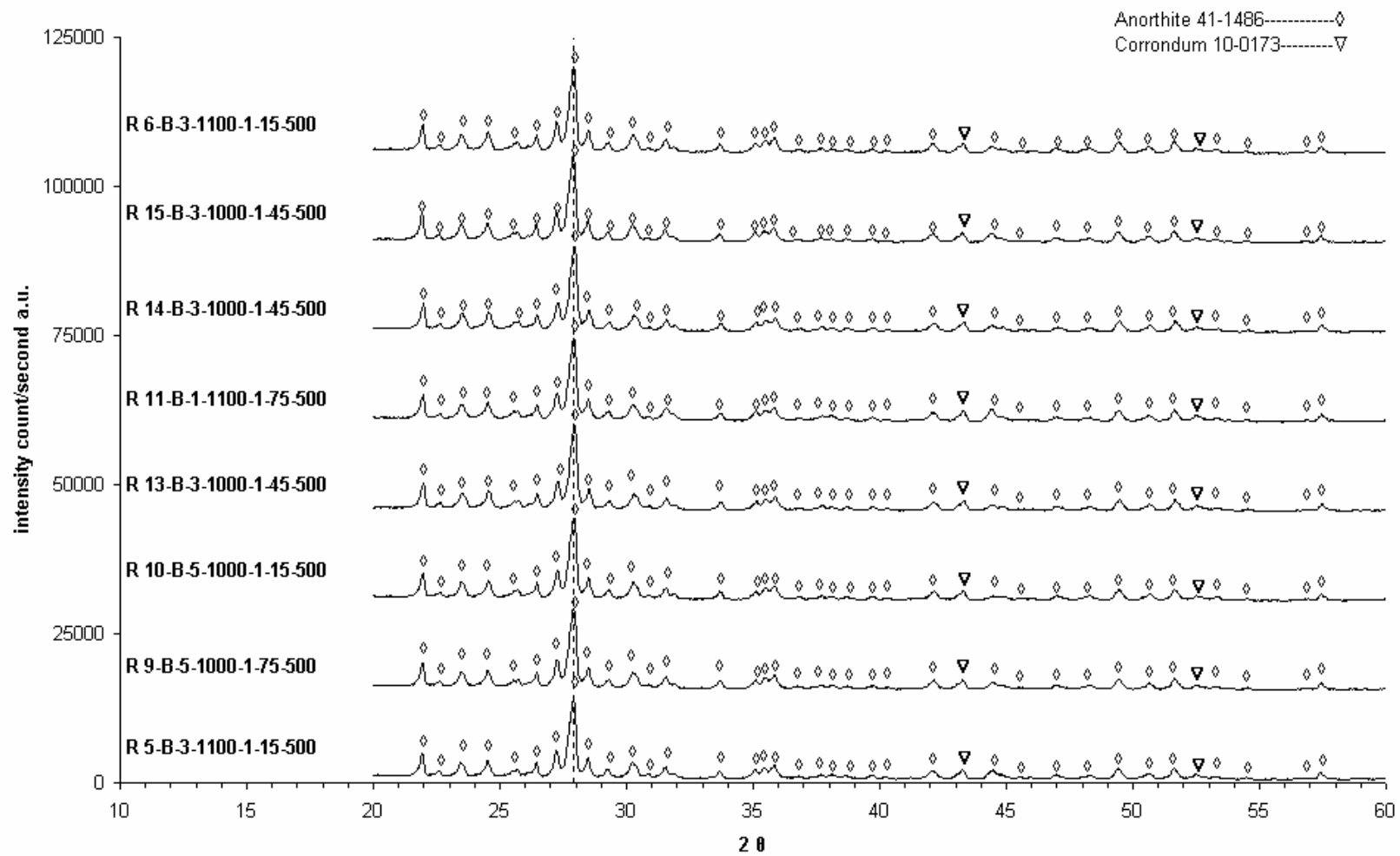


Figure 4.3. XRD patterns of the Box-Behnken response surface design (1)

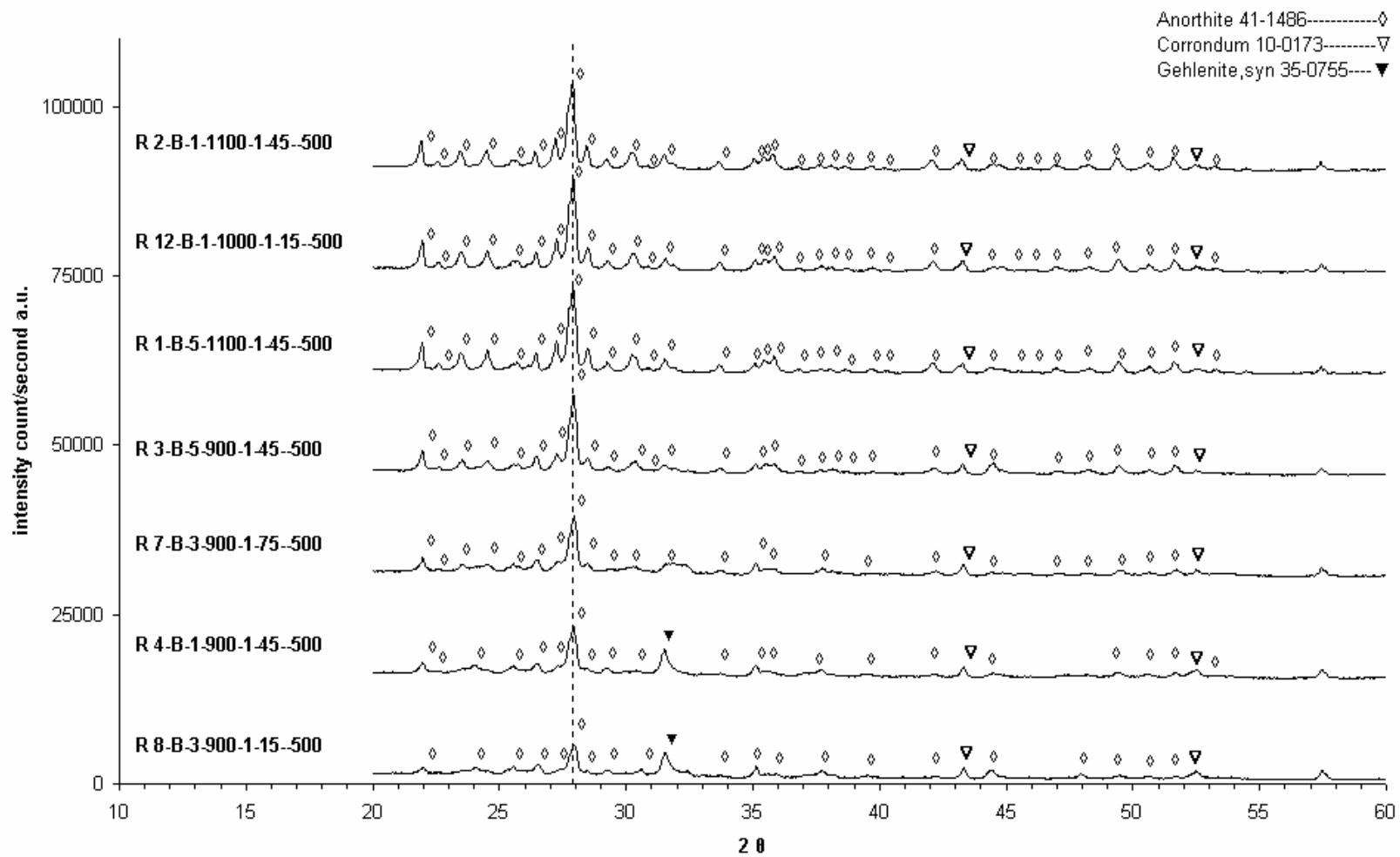


Figure 4.4. XRD patterns of the Box-Behnken response surface design (2)

Table 4.5. The responses of experiments for Box-Behnken design

Sample Labels	Coded run points			Response peak Intensity height
	Sintering temperature	Additive amount	Grinding Time	
	A	B	C	
R1-B-5-1100-1-45-500	+1	+1	0	1300
R2-B-1-1100-1-45-500	+1	-1	0	1343
R3-B-5-900-1-45-500	-1	+1	0	1209
R4-B-1-900-1-45-500	-1	-1	0	806
R5-B-3-1100-1-75-500	+1	0	+1	1349
R6-B-3-1100-1-15-500	+1	0	-1	1473
R7-B-3-900-1-75-500	-1	0	+1	940
R8-B-3-900-1-15-500	-1	0	-1	564
R9-B-5-1000-1-75-500	0	+1	+1	1396
R10-B-5-1000-1-15-500	0	+1	-1	1411
R11-B-1-1000-1-75-500	0	-1	+1	1435
R12-B-1-1000-1-15-500	0	-1	-1	1337
R13-B-3-1000-1-45-500	0	0	0	1428
R14-B-3-1000-1-45-500	0	0	0	1476
R15-B-3-1000-1-45-500	0	0	0	1464

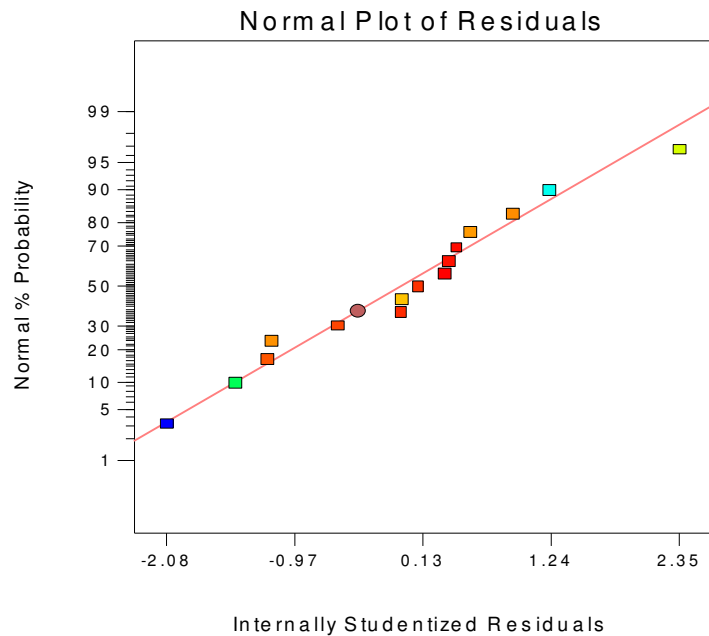


Figure 4.5. Normal probability plot for Box-Behnken design

The statistical analyses results (ANOVA table) for the response surface design of anorthite synthesis data are given in Table 4.6. The sum of squares was used as a measure of overall variability in the data and the value of 9.471E+005 indicated that the variation in the experiment data was very large. The model F-value of 9.88 implies that the model was significant. There was only a 0.36 % chance that a "Model F-Value" this large occurs due to noise. The significance of each term on the anorthite synthesis was shown by the values in column "Prob > F". Values of "Prob > F" less than 0.05 indicate that model terms were significant at the 95% confidence level. In other words we were 95% confident that the particular effect was significant. According to ANOVA table, A (sintering temperature) had the minimum Prob > F value as it was determined in screening experiments. Also, the statistical analyses for Box-Behnken design results that sintering temperature had second order effect, which had a Prob > F value of 0.0018, on formation of anorthite phase.

The Design Expert 7.0. software output for Box-Behnken response surface design is given in Table 4.7. The model R<sup>2</sup> value was 0.9081. That was about 91 percent of variability in the anorthite synthesis was explained by factor A (sintering temperature) and its second order. The Adeq Precision value was 8.996. This value measures the signal to noise ratio where, a ratio greater than 4 is desirable. So, the value of 8.996 indicated an adequate signal and this model can be used to navigate the design space.

Table 4.6. ANOVA table for the Box-Behnken response surface design

Source	Sum of Squares	df	Mean Square	F Value	p-value Prob > F	
<b>Model</b>	9.471E+005	7	1.353E+005	9.88	0.0036	significant
<b>A-Sintering Temperature</b>	4.729E+005	1	4.729E+005	34.54	0.0006	significant
<b>B- Additive Amount</b>	19701.13	1	19701.13	1.44	0.2693	
<b>C- Grinding Time</b>	14112	1	14112.00	1.03	0.3438	
<b>AB</b>	49729.00	1	49729.00	3.63	0.0983	significant
<b>AC</b>	62750.25	1	62750.25	4.58	0.0695	significant
<b>BC</b>	3192.25	1	3192.25	0.23	0.6439	
<b>A<sup>2</sup></b>	3.248E+005	1	3.248E+005	23.72	0.0018	significant
<b>Residual</b>	95826.84	7	13689.55			
<b>Lack of Fit</b>	95098.17	5	19019.63	52.20	0.0189	significant
<b>Pure Error</b>	728.67	2	364.33			
<b>Cor Total</b>	1.043E+006	14				

Table 4.7. Design Expert 7.0. software output for Box-Behnken response surface design

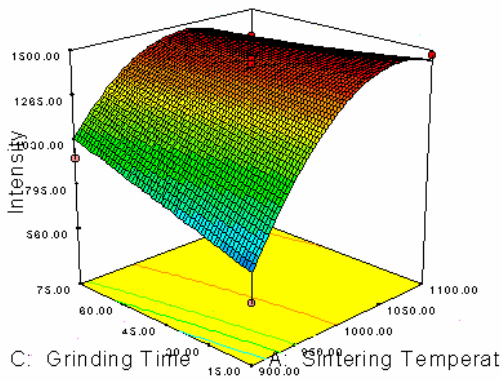
Std. Dev.	117.00	R Squared	0.9081
Mean	1261.27	Adj R Squared	0.8162
C.V. %	9.28	Pred R Squared	0.3593
PRESS	6.682E+005	Adeq Precision	8.996

The prediction equation shown (equation 4.1) below was generated by Design Expert 7.0 for coded factors. Coded factors A, B and C are sintering temperature, additive amount and grinding time, respectively. Figure 4.6 shows the predicted responses which were estimated from the prediction equation (equation 4.1), and their comparison with the observed responses.  $R^2$  value of this plot was 0.908. According to this result, it can be concluded that the prediction equation generated by Design Expert 7.0 was good at estimating the response values and this equation can be used for generating the response surfaces. The 3D response surfaces and design cube are given in Figure 4.7. The response surface can be generated for two factors so the other third factor was fixed at its middle level. For example, additive amount was fixed at 3 wt% for the response surface of sintering temperature against grinding time. It was found from both the ANOVA table (Table 4.6) and the response surface plots (Figure 4.7) that the effect of heating temperature was so strong that the effects of other factors was far less significant.

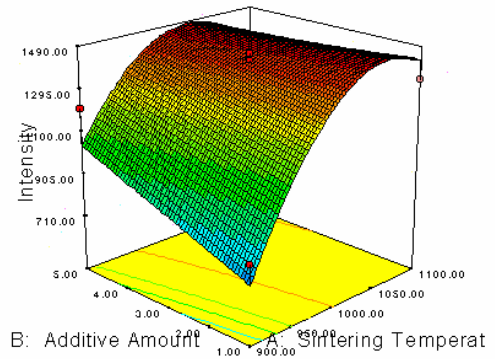
Final Equation in Terms of the Coded Factors :

$$\text{Intensity} = 1418.57 + 243.12 * A + 49.62 * B + 42.00 * C - 111.50 * A * B - 125.25 * A * C - 28.25 * B * C - 294.95 * A^2 \quad (4.1)$$

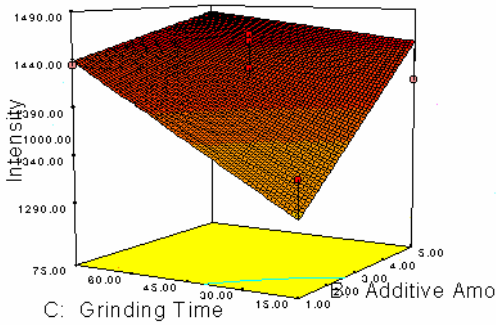




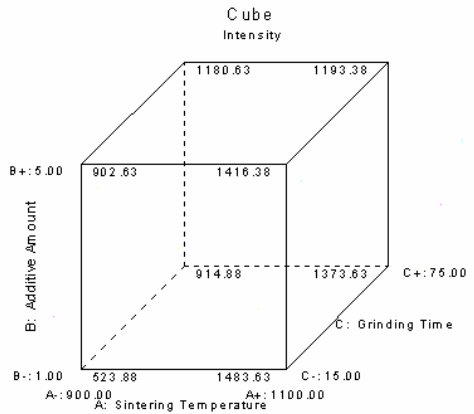
(a) A vs C, B = 3 wt%



(b) A vs B, C = 45 minutes



(c) B vs C, A = 1000 °C



(d) design cube

Figure 4.7. Response surfaces and design cube

The response surface plots showed that as the sintering temperature (factor A) increased anorthite phase formation also was increased (Figure 4.7.a – Figure 4.7.b). The effect of additive amount (factor B) and grinding time (factor C) had little influence on the response which was slightly more pronounced at low heating temperatures (Figure 4.7.c). The design cube shown in Figure 4.7.d represents the predicted responses for the corner points of cube while these points were not actual run points. According to the results of the software, the levels of factors at the optimum operation point listed in Table 4.8. The maximum response was predicted at this point according to the results of response surface analysis.

Table 4.8. The levels of factors at the optimum operation point

<b>Sintering temperature</b>	1038.91
<b>Additive amount</b>	4.43
<b>Grinding time</b>	23.91
<b>Prediction</b>	1491.97

#### 4.1.4. Effect of Grinding Speed and Temperature on Anorthite Synthesis

In this study, ladder type experiments were performed on several batches in order to understand the effect of grinding on anorthite phase formation. Ladder type experiments mean that running experiments for levels of a factor and fixing other factors at a constant level. The grinding speed was an important factor according to the Plackett-Burmann screening design. So, grinding speed was selected by changing the variable from 100 rpm to 500 rpm. The samples analyzed in this study were G11-B-1-800-1, G11-B-1-900-1 and G12-B-1-11000-5. The experiments studied in this section are listed in Table 4.9.

Table 4.9. Samples studied for effect of grinding analysis

<b>Samples fired at 800 °C</b>	<b>Samples fired at 900 °C</b>	<b>Samples fired at 1000 °C</b>
G11-B-1-800-1-60-100	G11-B-1-900-1-60-100	G12-B-1-11000-5-60-100
G11-B-1-800-1-60-200	G11-B-1-900-1-60-200	G12-B-1-11000-5-60-200
G11-B-1-800-1-60-300	G11-B-1-900-1-60-300	G12-B-1-11000-5-60-300
G11-B-1-800-1-60-400	G11-B-1-900-1-60-400	G12-B-1-11000-5-60-400
G11-B-1-800-1-60-500	G11-B-1-900-1-60-500	G12-B-1-11000-5-60-500

The XRD patterns of samples fired at 800 °C are represented in Figure 4.8. Anorthite phase was not observed in these samples. From XRD patterns corundum, quartz, calcium silicate and calcium aluminum borate was detected as main phases with a minor phase of calcium borate. Sintering temperature of 800 °C was not enough for

anorthite crystallization. Increasing grinding speed resulted in a decrease in peak heights of quartz and calcium aluminum borate phases and promoted the formation of calcium silicate

The XRD patterns of samples, having the same parameter configurations like the samples in Figure 4.8 but having sintering temperature of 900 °C, are shown in Figure 4.9. The anorthite phase formation was not observed in sample G11-B-1-900-1-60-100. The XRD pattern shows that the dominant phases in this sample were corundum and gehlenite with minor phases of calcium silicate and quartz. Increasing grinding speed from 100 rpm to 200 rpm resulted in anorthite phase formation with small amount of corundum phase. The existence of corundum phase is due probably to missing the perfect mix stoichiometry. Further increase of the grinding speed promoted anorthite crystallization. The peaks became narrower and their intensities increased with increasing grinding speed.

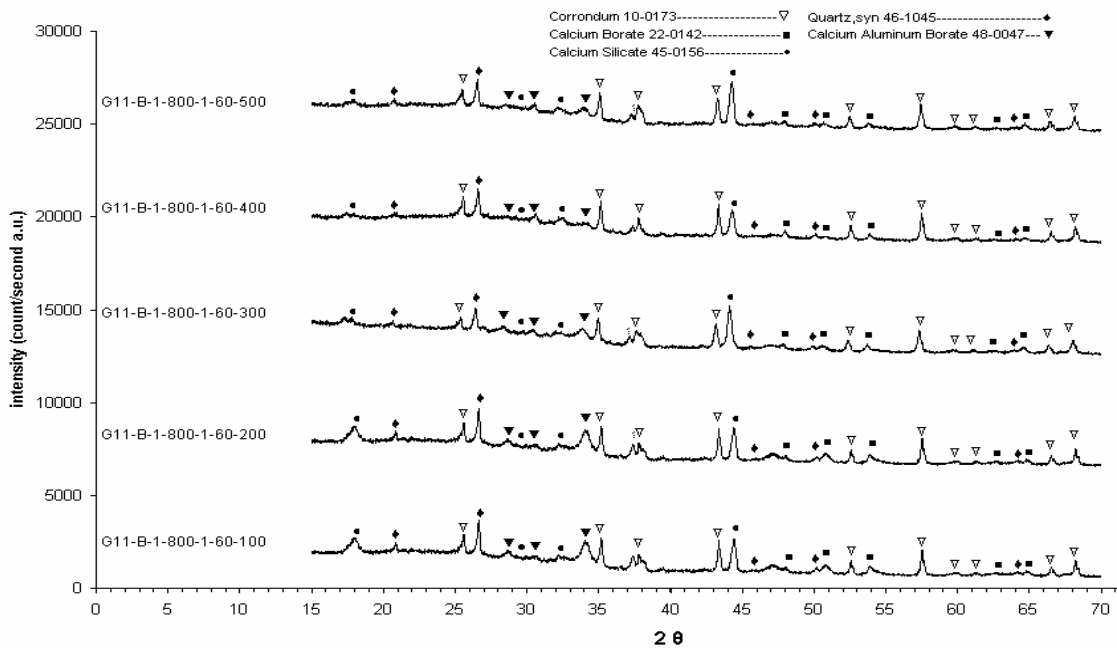


Figure 4.8. The XRD patterns of samples fired at 800 °C that were ground at different speeds

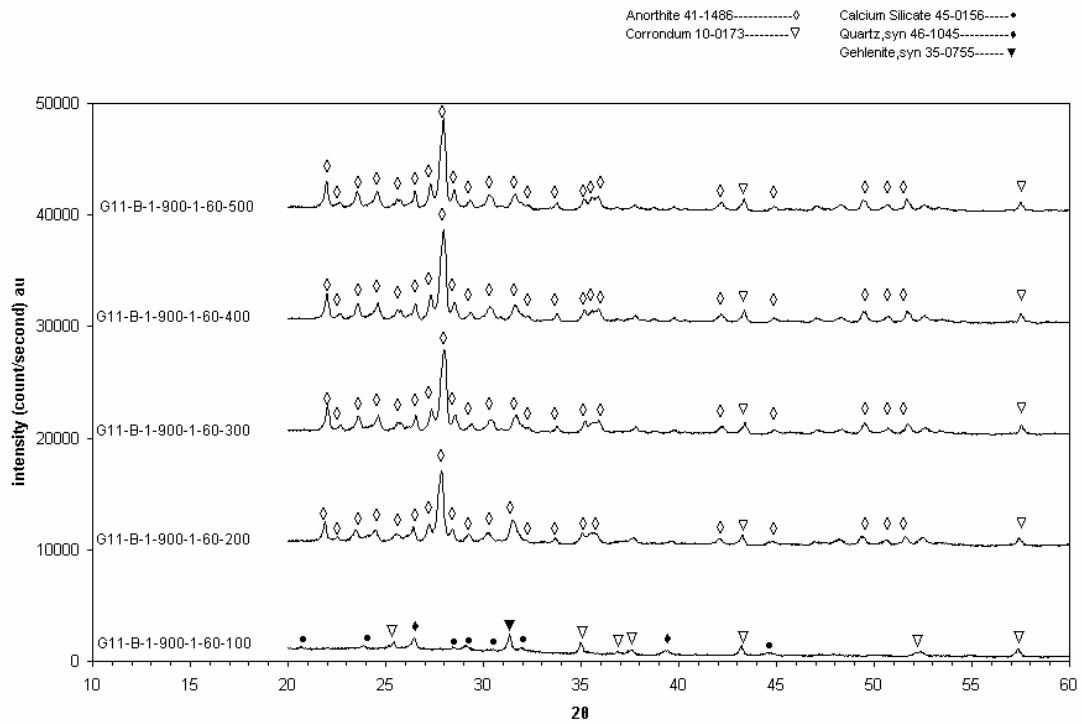


Figure 4.9. The XRD patterns of samples fired at 900 °C that were ground at different speeds

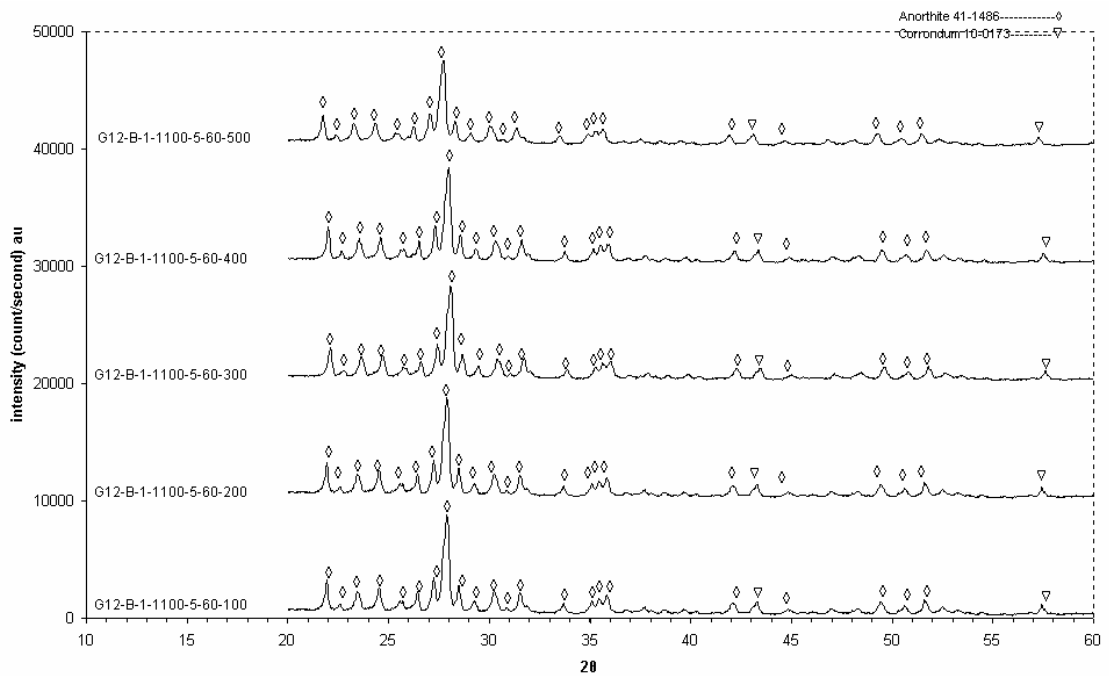


Figure 4.10. The XRD patterns of samples fired at 1100 °C that were ground at different speed

In order to investigate the effect of grinding speed at high sintering temperature such as 1100 °C five samples were studied. Each sample was identical by means of compositions and production routes but they were ground at different grinding speeds that varied from 100 rpm to 500 rpm. The XRD results are illustrated in Figure 4.10. Anorthite and minor amount of corundum phase was detected in all samples. However, in this case increasing the grinding speed did not affect the crystallization like it was observed in samples that were fired at 800 °C and 900 °C. This was probably due to the fact that there was enough thermal energy given by solid state sintering to the samples for anorthite phase formation and the energy exerted by grinding became less important.

#### **4.1.5. Effect of Alumina Source on the Anorthite Synthesis**

In this section effect of alumina source is investigated. The sample R7-B-900-1-75-500 is compared with sample A7-B-900-1-75-500. These two samples were identical and the only difference between them was the source of alumina. First batch was prepared with  $\text{Al}_2\text{O}_3$  and the second was prepared with  $\text{Al}(\text{OH})_3$ . The XRD results are given in Figure 4.11. Anorthite and the small amount of corundum phase were detected in both samples. As can be seen from the figure the sample that was prepared with  $\text{Al}(\text{OH})_3$  had narrower peaks and its had larger peak intensities. This result is reasonable that  $\text{Al}(\text{OH})_3$  is more reactive than  $\text{Al}_2\text{O}_3$ . In other words  $\text{Al}(\text{OH})_3$  gets into reaction at lower temperatures than  $\text{Al}_2\text{O}_3$ . Even the fact that in our experiments most of the alumina came from Sivas kaolin ( $\text{Al}_2\text{O}_3 \cdot 2\text{SiO}_2 \cdot 2\text{H}_2\text{O}$ ), getting the needed alumina from  $\text{Al}(\text{OH})_3$  promoted anorthite crystallization.

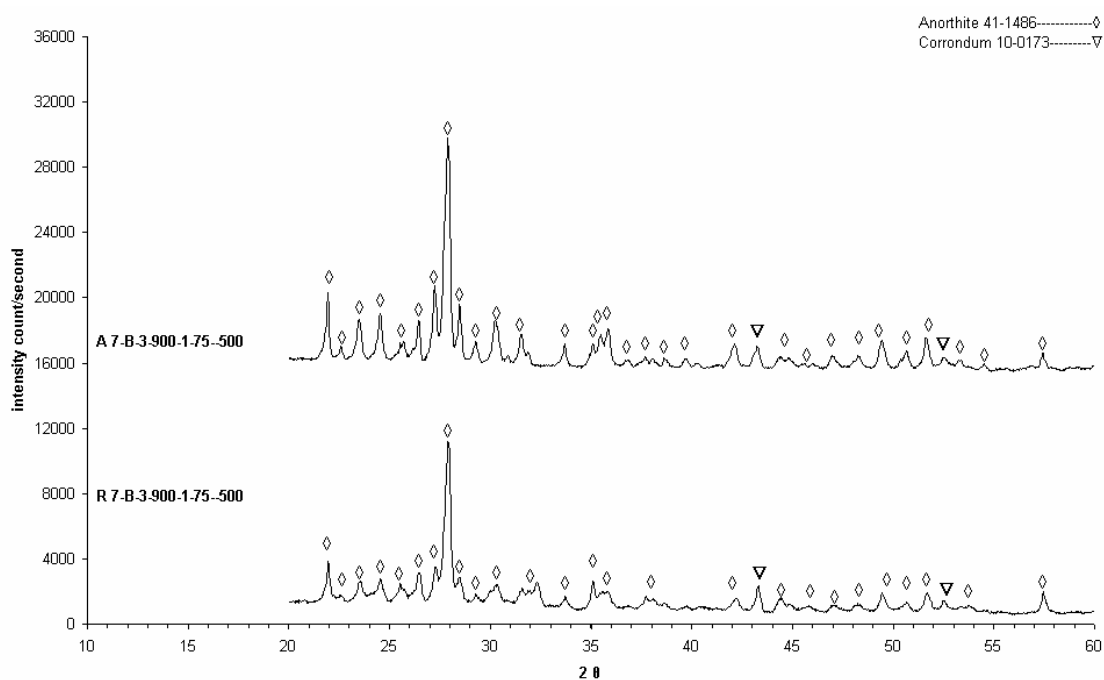


Figure 4.11. The XRD patterns of samples that had different Al<sub>2</sub>O<sub>3</sub> sources

#### 4.1.6. Effect of Grinding Time on Anorthite Synthesis

The effect of grinding time on anorthite synthesis was also investigated. The samples investigated for this analysis were prepared with 3 wt% boric acid addition and heated at 900 °C for 1 hour. The grinding speed was held constant at 500 rpm and the only difference between the batches was the grinding time. The results are presented in Figure 4.12. Increasing the grinding time from 15 minutes to 45 minutes enhanced anorthite formation. However, increasing the grinding time from 45 minutes to 90 minutes did not much increase the anorthite phase formation.

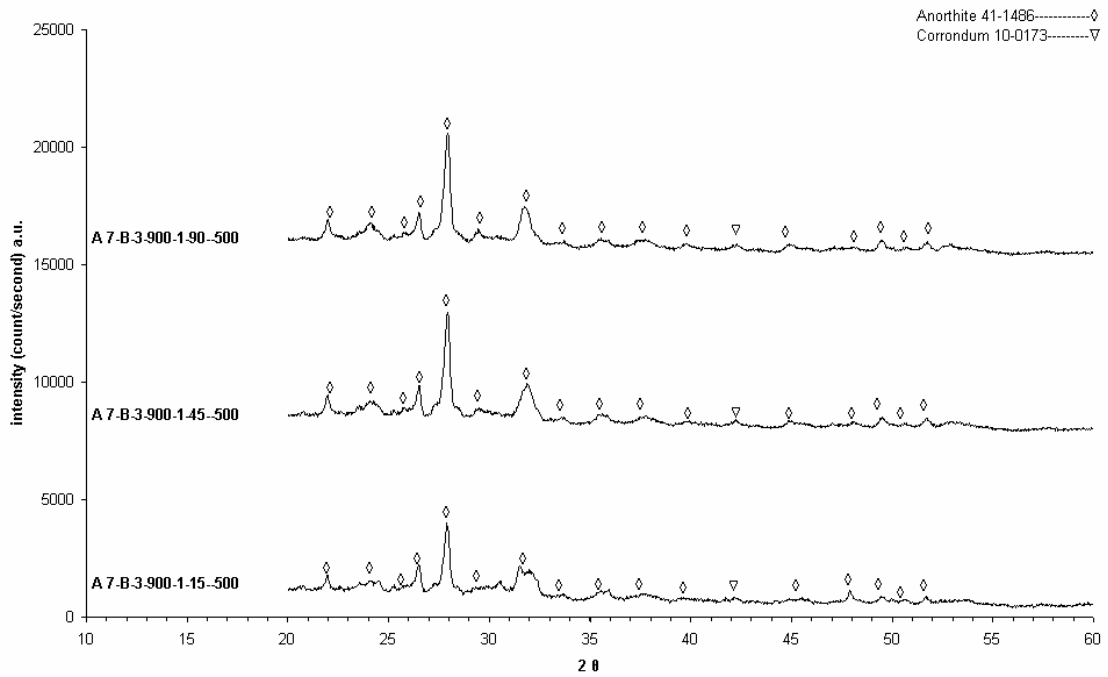


Figure 4.12. The XRD patterns of samples that were ground for different grinding durations

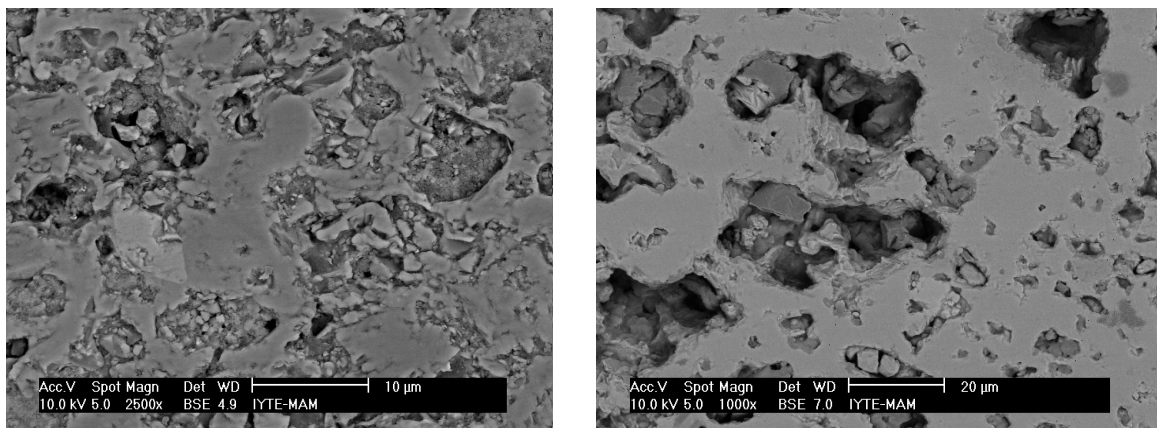
## 4.2 Microstructural Analyses (SEM)

In order to investigate the microstructural status of the synthesized pellets, SEM analyses were performed on polished cross sections of specimens. The secondary electron images of selected powder samples is presented in Figures 4.13 - 4.15.

Effect of sintering temperature and soak time on microstructure of anorthite were inspected by using SEM on backscatter electron images (BSE) of polished sections of selected samples. The general view of the samples are shown in Figure 4.13-a and Figure 4.13-b. The samples S11-B-1-900-1-60-100 and S12-B-1-1100-5-60-100 displayed bi-modal pore size distributions. In EDX analyses, it was detected that light grey areas contained a higher proportion of alumina and silica. According to the EDX analyses the dark grey areas were composed of calcium aluminum and a small proportion of silica.

The SEM micrographs of sample R13-B-3-1000-1-45-500 is given in Figure 4.14. The pores were in angular shape and their size varied between 5-30  $\mu\text{m}$ . A careful observation of Figure 4.14b revealed that the structure was composed of needle-like light

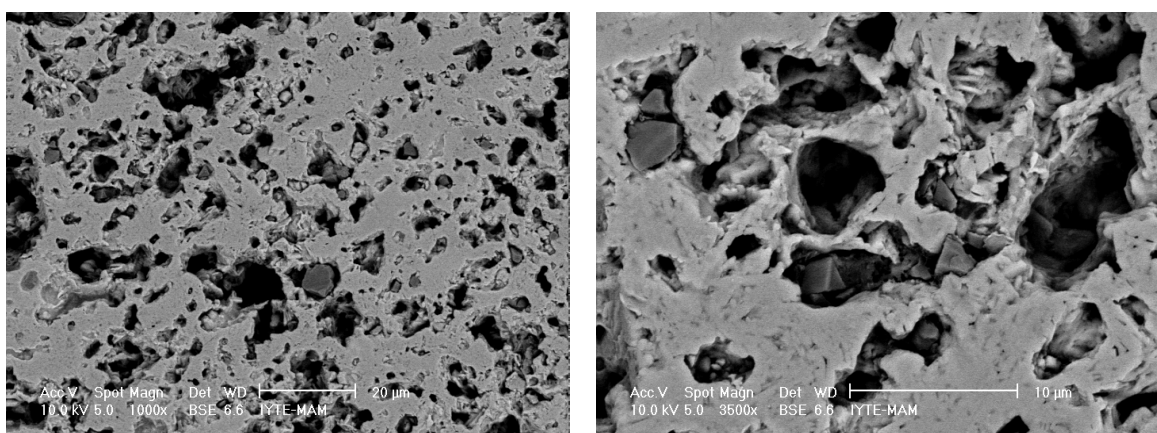
grey areas having surrounded by a glassy phase. These structures had an average size of 2.55  $\mu\text{m}$ . The EDX analyses carried out in order to determine chemical compositions of these needle-like structures. According to the results, these structures were composed of 24.95 wt% aluminum, 19.36 wt% silicon and 11.16 wt% calcium elements. These needle-like shapes were more clearly observed in the SEM micrographs of sample R6-B-3-1100-1-15-500, which is shown in Figure 4.15. The glassy matrix which was surrounded by the needle like structures is shown in more detail in Figure 4.15 b. In fact, this phase had nearly the same chemical composition like the needle-like structures.



(a) S11-B-1-900-1-60-100

(b) S12-B-1-1100-5-60-100

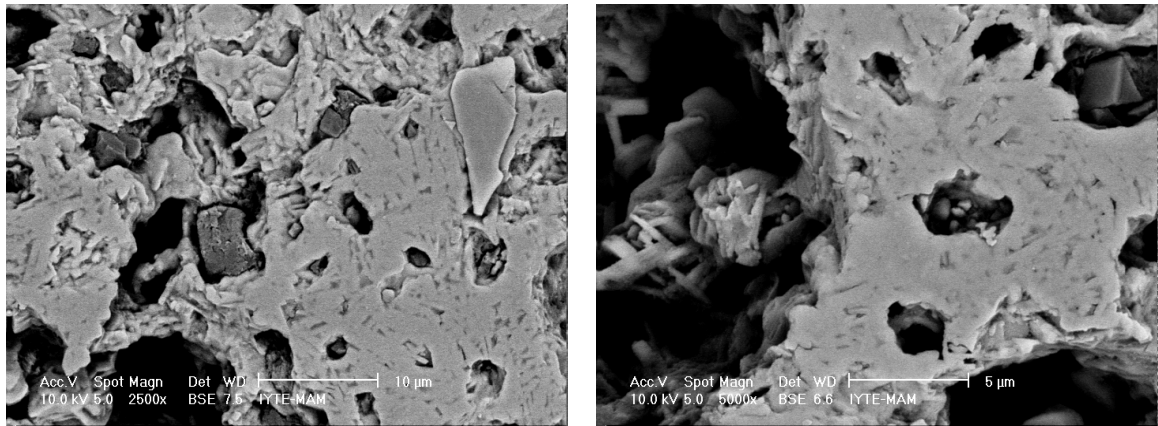
Figure 4.13. SEM micrographs of specimens heated at different temperatures and soak times.



(a) 1000x

(b) 3500x

Figure 4.14. SEM micrographs of sample R13-B-3-1000-1-45-500



(a) 2500x

(b) 5000x

Figure 4.15. SEM micrographs of sample R6-B-3-1100-1-15-500

### 4.3. Density and Porosity Evaluation

Density and porosity measurements of heated pellets are given in Table 4.10. A maximum of 75.6 % of the theoretical density was achieved for anorthite synthesis in sample R4-B-1-900-1-45-500. This result is reasonable because of the porous structure formed in the pellets by loss of water and carbon dioxide formation from the raw materials during heating.

The amount of apparent porosity was constant in most of the samples and its value varied between 30-40 % in the samples. Addition of a calcination step and recompaction of these calcined powders will promote the density and decrease the porosity levels.

Table 4.10. Archimedes density of anorthite pellets

	Samples	Apparent Porosity. %	Water Absorption. %	Bulk Density. g/cm <sup>3</sup>	Theoretical Density. %
1	R1-B-5-1100-1-45-500	38.8	22.9	1.69	61.2
2	R2-B-1-1100-1-45-500	32.6	17.3	1.88	68.1
3	R3-B-5-900-1-45-500	38.5	25.4	1.52	55.1
4	R4-B-1-900-1-45-500	15.1	8.2	2.09	75.6
5	R5-B-3-1100-1-75-500	33.6	18.7	1.80	65.2
6	R6-B-3-1100-1-15-500	25.4	15.7	1.80	65.3
7	R7-B-3-900-1-75-500	53.7	37.5	1.50	54.4
8	R8-B-3-900-1-15-500	38.9	23.1	1.69	61.1
9	R9-B-5-1000-1-75-500	44.0	28.5	1.55	56.0
10	R10-B-5-1000-1-15-500	43.0	27.5	1.57	56.7
11	R11-B-1-1000-1-75-500	35.6	19.6	1.82	65.8
12	R12-B-1-1000-1-15-500	36.6	20.5	1.79	64.8
13	R13-B-3-1000-1-45-500	41.1	24.9	1.65	59.7
14	R14-B-3-1000-1-45-500	42.3	26.2	1.61	58.4
15	R15-B-3-1000-1-45-500	41.9	25.8	1.62	58.8
16	S1-B-5-900-1-15-500	38.9	23.7	1.64	59.4
17	S2-C-1-900-1-15-100	41.7	25.7	1.63	58.9
18	S3-B-1-1100-5-15-500	31.8	16.9	1.88	68.2
19	S4-C-1-900-5-15-500	35.4	19.6	1.80	65.3
20	S5-B-5-1100-1-15-100	39.2	23.9	1.64	59.5
21	S6-C-1-1100-1-60-500	24.7	12.3	2.02	73.2
22	S7-C-5-1100-1-60-500	30.2	15.7	1.93	69.9
23	S8-C-5-900-5-60-100	46.9	33.3	1.45	52.6
24	S9-B-5-900-5-60-500	37.7	22.5	1.68	60.8
25	S10-B-5-900-1-15-500	39.7	31.8	1.49	54.0
26	S11-B-1-900-1-60-100	34.1	18.8	1.82	65.9
27	S12-B-1-1100-5-60-100	37.9	21.5	1.76	63.8
29	A7-B-3-900-1-75-500	38.9	23.7	1.64	59.4

## CHAPTER 5

### CONCLUSIONS

In this study, the effects of heating temperature, soaking time, amount and type of additives and mechanochemical treatment on synthesis of anorthite ceramics were investigated. The purpose was to decrease the formation temperature of anorthite. The factors were examined by using statistically designed set of experiments (Plackett-Burman screening experiment design) because there were many variables to choose and the more important factor effects were needed to be screened out. As a result of the screening experiments, the effects of heating temperature, grinding speed, additive amount and soak time were found to be more significant. This choice was done based on both hand calculations and software computations using analysis of variance method.

In the second set of experiments, response surface methodology was employed by using Box-Behnken design to investigate the effects of heating temperature, additive amount and grinding time on anorthite synthesis. There were three different levels for each parameter in this set of experiments. The response surfaces were obtained from these experiments using the model polynomial equation. The effect of temperature was more pronounced than grinding time and additive amount. There was not much of an interaction between the parameters.

In the final set of experiments, the effects of different alumina sources, sintering temperature, grinding speed and grinding time, were investigated with ladder experiments. The effect of mechanical treatment on anorthite synthesis was much less significant compared to the effect of heating temperature but was nevertheless statistically significant. The same was true for the effect of grinding time. The use of  $\text{Al}(\text{OH})_3$  instead of calcined alumina as a source of  $\text{Al}_2\text{O}_3$  promoted anorthite formation. The combined effect of additive usage and high speed grinding anorthite sintering temperature decreased down to 900 °C. A relative density of 75.6 % of the theoretical density was obtained. Microstructures of the heated pellets were also observed using SEM to find out that the structure was porous. Anorthite phase was successfully produced as a result of this study.

Future study of the subject can involve the effect of a more intense grinding along with the use of a less alumina rich clay combined with a greater proportion of aluminum hydroxide. This latter additive can perhaps help obtain lower synthesis temperatures. Different types of diffusion aids like  $K_2O$  and  $Li_2O$  can also be employed.

## REFERENCES

- Alcoa Industrial Chemicals Europe. 2001. "Calcined and Reactive Aluminas for the Ceramic Industry Product Data", Frankfurt.
- Bergeron C. G. and Risbud S.H., 1984. "Introduction to Phase Equilibria in Ceramics" American Ceramic Society (Westerville, Ohio), pp. 143-147.
- Boldyrev V.V. and Tkacova K. 2000. "Mechanochemistry of Solids: Past, Present and Prospects", *J. Materials Synthesis and Processing*. Vol.8, No.3, pp.121-132.
- Boudchicha M. R., Achour S., Harabi A. 2001. "Crystallization and sintering of cordierite and anorthite based binary ceramics", *Journal of Materials Science Letters* Vol.20, No.3, pp.215-217.
- Çakır Ö., 1981. "Production of Cordierite from Domestic Raw Materials" M. Sc. Thesis, Middle East Technical University, Ankara
- Deer W. A., Howie R. A., and Zussman J., 1963. *Rock-Forming Minerals*, Vol. 4; pp.94-165. (John Wiley & Sons, Inc., New York), pp. 42-71.
- Gdula R.A. 1971. "Anorthite Ceramic Dielectrics", *Ceramics International*. Vol.50, No.6 pp.143-146.
- Guechi A., Achour S., Harabi A., 2004. "Effect temperature and Na<sub>2</sub>CO<sub>3</sub> additions on sintering and crystallization of anorthite", *Key Engineering Materials*. Vols. 64-268, pp. 257-260.
- Greig J. W., 1927. "Immiscibility in silicate melts", *American Journal of Science*. 5th Ser., Vol. 13, No.4, pp. 1-41 and 133-154.
- Harris H. and Lautenberger W., 1976. "Strategy of Experimentation", (E.I.Dupont de Nemours & Co. Inc.) Short Course Notes, pp.29-45
- Kingery W.D., 1975. "Introduction to Ceramics" (John Wiley & Sons, Inc.), pp. 79-81 and 498-501.
- Kırıkoğlu M. S., Sümer A., Özkan S. G., and Özden G., 2004. "Investigation of Some Physical and Chemical Properties With Respect to Processing of Kaolin Samples from Sivas Deposits in Turkey", *Key Engineering Materials*. Vol.264-268, No.3, pp.1423-1426.
- Knickerbocker S.H., Kumar A.H., Herron L.W., 1993. "Cordierite glass-ceramics for multilayer ceramic packing", *American Ceramic Society Bulletin*. Vol. 72, No. 1, pp. 90-95.

- Kobayashi Y and Kato E., 1994. "Low temperature fabrication of anorthite ceramics", *Journal of American Ceramic Society*. Vol.77, No.3, pp. 833-34
- Kostic E., Kiss S., Boskovic S. and Zec S., 1997. "Mechanical activation of the gamma to alpha transition in  $Al_2O_3$ ", *Powder Technology*. Vol.8, No.4, pp.49-54
- Lee S. and Kim G., 2002. "Characteristics and densification behavior of anorthite powder synthesized by a solution process employing a polymer carrier.", *Journal of Ceramic Processing Research*. Vol. 3, No. 3, pp. 136-140
- Leigh III H. D. and Towe C. A., 1987. "Use of a Screening Experimental Design to Develop a High  $Al_2O_3$  Casting Slip", *American Ceramic Society Bulletin*. Vol.66, No. 5, pp. 86-89.
- Mergen A. and Aslanoglu Z., 2003. "Low-temperature Fabrication of Anorthite Ceramics From Kaolinite and Calcium Carbonate with Boron Oxide Addition", *Ceramic International* Vol.29, No.5, pp.667-670.
- Mergen A., Kayed T.S., Bilen M., Qasrawi A.F. and Gürü M.,-2004 "Production of Anorthite from Kaolinite and  $CaCO_3$  via Colemanite", *Key Engineering*. Vol. 264-268, No. 4, pp. 1475-1478
- Montgomery D. C., 2005. "Design and Analysis of Experiments", 6th Edition, (John Wiley & sons, Inc., USA), pp. 318-322 and 405-458
- Muan A. and Osborn E. F., 1964. "Phase Equilibria among oxides in steel making", (Addison-Wesley Publishing Company Inc., USA), pp 214-225.
- Nesse W. D., 1991. "Introduction to optical mineralogy" 2<sup>nd</sup> edition, (Oxford University Press, New York, USA), pp. 196-198
- Okada K., Watanabe N., Jha K., Kameshima Y., Yasumori A., MacKenzie K., 2003. "Effects of grinding and firing conditions on  $CaAl_2SiO_8$  phase formation by solid-state reaction of kaolinite with  $CaCO_3$ .", *Applied Clay Science*. Vol. 23, No.1, pp. 329-336
- Rankin G. A., Wright F. E., 1915. "The ternary system  $CaO-Al_2O_3-SiO_2$  ", *American Journal of Science*. 4th Ser., Vol. 39, No.3, pp. 1-52.
- Rojac T., Kosec M., Malič B., Holc J., 2006. "The application of a milling map in the mechanochemical synthesis of ceramic oxides", *Journal of the European Ceramic Society*. Vol.4, No.2, pp. 826-832.
- Standard Test Methods for Apparent Porosity, Water Absorption, Apparent Specific Gravity, and Bulk Density of Burned Refractory Brick and Shapes by Boiling Water, ASTM Designation: C20-87, Annual Book of ASTM Standards, Vol., (1987).

- Steinike U. and Tkacova K., 2000. "Mechanochemistry of Solids-Real Structure and Reactivity", *J. Materials Synthesis and Processing*. Vol.8, No.3, pp. 197-203.
- Traoré K., Kabré T., Blanchart P., 2003. "Gehlenite and anorthite crystallization from kaolinite and calcite mix.", *Ceramics International*. Vol. 29, No.4, pp.377-383
- WEB\_1, 2006. cnr.berkeley's web site 10/06/2006. [ttp://cnr.berkeley.edu/classes/espm-121/soilmineralogy.html](http://cnr.berkeley.edu/classes/espm-121/soilmineralogy.html).
- Yalamaç E. and Akkurt S., 2006. "Additive and intensive grinding effects on the synthesis of cordierite", *Ceramics International*. Vol.32, No.3, pp.825-832
- Yang C. and Cheng C., 1998."The sintering characteristics of MgO-CaO-Al<sub>2</sub>O<sub>3</sub>-SiO<sub>2</sub> composite powder made by sol-gel method", *Ceramic International*. Vol.24, No.3, pp.243-247.
- Yang C. and Cheng C., 1999. "The influence of B<sub>2</sub>O<sub>3</sub> on the sintering of MgO-CaO-Al<sub>2</sub>O<sub>3</sub>-SiO<sub>2</sub> composite glass powder", *Ceramic International*. Vol.25, No.2, pp. 383-387.